

# **Ph.D. Thesis**

**Generation of isoform-specific monoclonal antibodies  
against human UDP-glucuronosyltransferases (UGTs) and  
tissue-specific expression of UGTs by epigenetic regulation**

**Drug Metabolism and Toxicology  
Department of Molecular Effects  
Division of Life Sciences  
Graduate School of Natural Science and Technology  
Kanazawa University**

<b>School registration No.</b>	<b>1123032309</b>
<b>Name</b>	<b>Shingo Oda</b>
<b>Supervisor</b>	<b>Miki Nakajima</b>



# LIST OF CONTENTS

## ABBREVIATIONS

### CHAPTER 1

General introduction	1
----------------------	---

### CHAPTER 2

Generation of specific monoclonal antibodies against human UDP-glucuronosyltransferase (UGT) 1A6, UGT1A8, UGT1A9, UGT1A10, UGT2B4, and UGT2B10 and evaluation of their protein levels in human tissues

Abstract	4
Introduction	5
Materials and methods	6
Results	10
Discussion	19

### CHAPTER 3

Epigenetic regulation is a crucial factor in the repression of UGT1A1 expression in the human kidney

Abstract	23
Introduction	24
Materials and methods	25
Results	29
Discussion	33

### CHAPTER 4

Tissue-specific expression of human UGT1A10 by epigenetic regulation

Abstract	36
Introduction	37

Materials and methods	37
Results	42
Discussion	50
<b>CHAPTER 5</b>	
Conclusion	54
REFERENCES	57
LIST OF PUBLICATIONS	67
ACKNOWLEDGEMENTS	68

## ABBREVIATIONS

ANOVA	Analysis of variance
5-Aza-dC	5-Aza-2'-deoxycytidine
Cdx2	Caudal type homeobox 2
ChIP	Chromatin immunoprecipitation
DMSO	Dimethyl sulfoxide
Dzneq	3-Deazaneplanocin A
Endo H	Endoglycosidase H
EZH	Enhancer of zeste
GAPDH	Glyceraldehyde-3-phosphate dehydrogenase
HNF	Hepatocyte nuclear factor
HPLC	High-performance liquid chromatography
miRNA	microRNA
PAGE	Polyacrylamide gel electrophoresis
PNGase F	peptide: <i>N</i> -glycosidase F
PRC	Polycomb repressive complex
PVDF	Polyvinylidene fluoride
RT	Reverse transcription
SDS	Sodium dodecyl sulfate
TSA	Trichostatin A
TSS	Transcription start site
UDP	Uridine 5'-diphosphate
UDPGA	UDP-Glucuronic acid
UGT	UDP-Glucuronosyltransferase
UTR	Utranslated region

# CHAPTER 1

## General introduction

UDP-Glucuronosyltransferases (UGTs, EC 2.4.1.17) are a family of phase II drug-metabolizing enzymes that play key roles in the metabolism of endogenous and exogenous compounds (Mackenzie et al., 2005). UGTs mediate the transfer of glucuronic acid from UDP-glucuronic acid (UDPGA) to hydroxyl, carboxyl, or amine groups of hydrophobic compounds, facilitating their elimination into bile and urine (Ritter, 2000). While glucuronidation usually inactivates biologically active molecules, there are exceptions such as morphine and retinoic acids, which are converted to pharmacologically active glucuronides (Formelli et al., 1996; Shimomura et al., 1971). Human UGTs are classified by evolutionary divergence into three subfamilies, including UGT1A, UGT2A, and UGT2B (Mackenzie et al., 2005). The human *UGT1A* gene cluster is located on chromosome 2q37 and contains multiple unique first exons, as well as the conserved exons 2-5, which can give rise to nine kinds of functional UGT1A isoforms, including UGT1A1, UGT1A3, UGT1A4, UGT1A5, UGT1A6, UGT1A7, UGT1A8, UGT1A9, and UGT1A10 (Ritter et al., 1992; Gong et al., 2001) (Fig. 1). The *UGT2A* and *UGT2B* genes are located on chromosome 4q13, encoding three and seven functional proteins, respectively. The UGT2A1 and UGT2A2 are formed by alternative splicing of variable first exons and common exons 2 to 6, likely the *UGT1A* gene, while UGT2A3 and each UGT2B are encoded by individual genes (Fig. 1).

The expression of UGT enzymes is subject to genetic polymorphism (Guillemette, 2003) and can be induced by various endogenous and exogenous compounds (Sutherland et al., 1993; Mackenzie et al., 2003). These features would be the possible reasons of interindividual variability of expression level and enzymatic activity, which may be associated with the interindividual variability of drug efficacy and toxicity. Thus, knowledge of tissue distribution and interindividual variability of UGT expression allows to predict pharmacokinetics of drugs. Recent studies uncovered the expression of UGTs in human tissues at mRNA levels (Izukawa et al., 2009; Court et al., 2012). However, there is little information on the protein expression levels of UGTs. One of the reasons for this is the limited availability of isoforms-specific antibody, since UGT isoforms share a high degree of amino acid similarity. In **chapter 2**, isoform-specific antibodies were prepared and subsequently tissue distribution and

interindividual variability in the enzyme expression of UGTs were investigated using these antibodies.

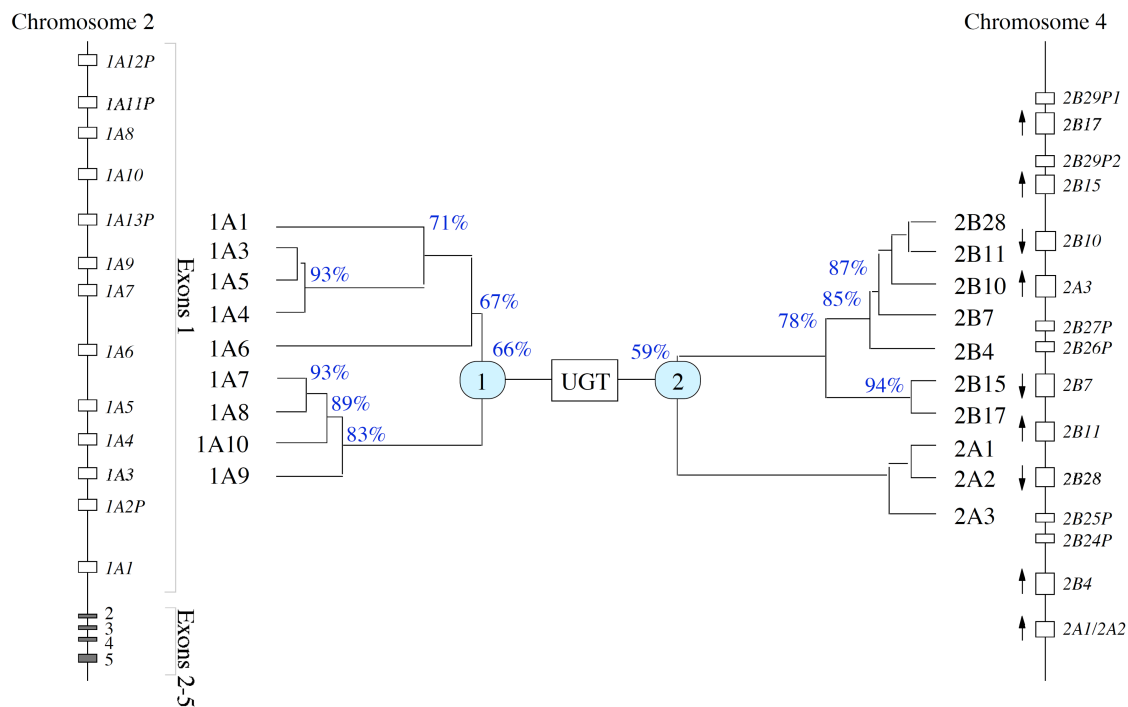


**Fig. 1.** Gene structure and phylogenetic tree of human UGT superfamily. The numbers in the phylogenetic tree represent amino acid identities. “P” after the gene number denotes a pseudogene. Arrows indicate the direction of transcription.

Human UGTs show tissue-specific expression. Although most UGTs are predominantly expressed in the liver, UGT1A7, UGT1A8, and UGT1A10 are exclusively expressed in the gastrointestinal tract (Strassburg et al., 1997, 1998a and 1998b). UGT1A1 is expressed in the liver, small intestine and colon, but not in the kidney (Nakamura et al., 2008; Ohno and Nakajin, 2009; Court et al., 2012). The expression of UGT2A1 and 2A2 are limited to the olfactory epithelium (Court et al., 2012). UGT2B7 is abundantly expressed in the liver, kidney, small intestine, and colon, whereas UGT2B10 is expressed only in the liver (Court et al., 2012). To understand the underlying mechanisms of the tissue-specific expression of UGTs, some studies were conducted with a focus on transcriptional regulation (Gardner-Stephen and Mackenzie, 2008; Mackenzie et al., 2010). It has been demonstrated that the intestine-specific transcription factor, caudal-type homeobox protein 2 (Cdx2), Sp1 and hepatocyte nuclear factor (HNF) 1 $\alpha$  regulate UGT1A8 and UGT1A10 expression in the

intestine (Gregory et al., 2004b). HNF1 $\alpha$  and Cdx2 cooperatively regulate UGT2B7 expression in the intestine, whereas HNF1 $\alpha$  and octamer transcription factor-1 cooperatively regulate its expression in the liver and kidney (Gregory et al., 2006). HNF1 $\alpha$  is also involved in the regulation of UGT1A1 expression in the liver (Bernard et al., 1999). Thus, knowledge of the transcriptional regulation of the tissue-specific expression of the UGTs is accumulating.

Nevertheless, a fundamental question that remains to be answered is defective expression of some UGTs in a given tissue even under the presence of *trans*-acting factor. For example, UGT1A1 and UGT1A10 are not expressed in the kidney and liver, respectively, even though HNF1 $\alpha$  is expressed in these tissues (Rey-Campos et al., 1991). This study sought to clarify the mechanisms underlying the defective expression of UGT1A1 and UGT1A10, with a focus on epigenetic regulation. It is well known that epigenetic mechanisms including DNA methylation and histone modification are key regulators of tissue-dependent gene expression (Shiota, 2004; Ohgane et al., 2008). In **chapters 3 and 4**, it was investigated whether DNA methylation of the promoter and histone modification might be determinants of the tissue-specific expression of human UGT1A1 and UGT1A10.

## CHAPTER 2

### **Generation of specific monoclonal antibodies against human UGT1A6, UGT1A8, UGT1A9, UGT1A10, UGT2B4, and UGT2B10 and evaluation of their protein levels in human tissues**

#### **ABSTRACT**

Glucuronidation is a major detoxification pathway of drugs and xenobiotics that is catalyzed by the UGT superfamily. Determination of the protein levels of the individual UGT isoforms in human tissues is required for the successful extrapolation of *in vitro* metabolic data to *in vivo* clearance. Most previous studies evaluating UGT isoform expression were limited to the mRNA level because of the high degree of amino acid sequence homology between UGT isoforms that has hampered the availability of isoform-specific antibodies. In this study, monoclonal antibodies against human UGT1A6, UGT1A8, UGT1A9, UGT1A10, UGT2B4, and UGT2B10 were generated using each UGT isoform-specific peptide. It was confirmed that these antibodies did not cross-react with the other human UGT isoforms. Using these antibodies, it was demonstrated that UGT1A6 and UGT1A9 proteins were expressed in both the kidney and the liver, but not in the small intestine, UGT2B4 and UGT2B10 were expressed only in the liver, and UGT1A10 was expressed only in the small intestine, that are consistent with previous reports of mRNA expression. In a panel of 20 individual human livers, the UGT1A6, UGT1A9, UGT2B4, and UGT2B10 protein levels exhibited 10-, 9-, 6-, and 7-fold variability, respectively. Interestingly, their relative protein and mRNA levels were not correlated, suggesting the importance of evaluating UGT isoform expression at protein levels. In conclusion, specific monoclonal antibodies against UGT1A6, UGT1A8, UGT1A9, UGT1A10, UGT2B4, and UGT2B10 were successfully generated and the distribution and relative expression levels of their protein in human tissues were evaluated. These antibodies would serve as a useful tool for further studies of UGTs to evaluate their physiological, pharmacological, and toxicological roles in human tissues.

## INTRODUCTION

Drug disposition and metabolism are key factors that determine interindividual differences in the pharmacokinetics of drugs. Therefore, the activities and the expression levels of drug-metabolizing enzymes and transporters have been a focus of interest for pharmacokinetic research for a long time and have been analyzed in attempts to evaluate individual differences of hepatic disposition and metabolism. Variability of UGT expression can be evaluated by measuring enzyme activity *in vitro* using specific substrates. However, substrates that are specifically metabolized by a single UGT isoform are limited because of the broad and overlapping substrate specificities of UGTs. Inappropriate selection of substrates may lead to misevaluation. An alternative approach is to measure mRNA levels of individual UGT isoforms. Indeed, earlier studies evaluated the interindividual difference in the expression or tissue distribution of UGT isoforms at the mRNA level (Izukawa et al., 2009; Ohno and Nakajin, 2009; Strassburg et al., 2000). However, it was reported that certain individual UGT mRNA levels correlate poorly with their respective protein levels (Izukawa et al., 2009, Ohtsuki et al., 2012). Therefore, it should be noted that the mRNA levels might not necessarily reflect the actual UGT protein levels. Immunochemical technique is the most conventional approach for the assessment of protein levels. However, this approach is limited by the specificity of available antibodies. Currently, specific antibodies for human UGT isoforms are only commercially available for UGT1A1 and UGT2B7. Antibodies against UGT1A4 and UGT1A9 are also available for purchase, but their specificity is not guaranteed. Because UGTs share a high degree of sequence similarity, it is a great challenge to generate an isoform-specific antibody against each UGT. Indeed, the antibody against UGT1A9 prepared by Girard et al. (2004) exhibits cross-reactivity against highly conserved enzymes UGT1A7, UGT1A8, and UGT1A10. In this study, specific monoclonal antibodies against human UGT1A6, UGT1A8, UGT1A9, UGT1A10, UGT2B4, and UGT2B10 were generated to evaluate the variability of UGT protein levels in human tissue samples by Western blot analysis.

## **MATERIALS AND METHODS**

### **Chemicals and reagents**

Recombinant human UGT1A1, UGT1A3, UGT1A4, UGT1A6, UGT1A7, UGT1A8, UGT1A9, UGT1A10, UGT2B4, UGT2B7, UGT2B10, UGT2B15, and UGT2B17 expressed in baculovirus-infected insect cells (Supersomes) as well as insect cell control Supersomes, human liver microsomes (a pooled sample,  $n = 50$ ) and human small intestine microsomes (a pooled sample,  $n = 6$ ) were purchased from BD Gentest (Woburn, MA). Human kidney microsomes (a pooled sample,  $n = 6$ ) was purchased from Tissue Transformation Technologies (Edison, NJ). Endoglycosidase H (Endo H) and peptide: *N*-glycosidase F (PNGase F) were purchased from New England Biolabs (Ipswich, MA). A goat anti-human hepatocyte nuclear factor (HNF) 1 $\alpha$  polyclonal antibody (C-19) and mouse anti- $\beta$ -actin monoclonal antibody (C-14) were purchased from Santa Cruz Biotechnology (Santa Cruz, CA). All the other reagents were of the highest grade commercially available.

### **Human tissues**

Human liver samples from 14 individual donors were supplied by the National Disease Research Interchange (NDRI, Philadelphia, PA) through the Human and Animal Bridging Research Organization (Chiba, Japan), and those from six Japanese donors were obtained from autopsy materials that were discarded after pathological investigation (Izukawa et al., 2009). Microsomes were prepared as described previously (Tabata et al., 2004). The use of the human livers was approved by the Ethics Committees of Kanazawa University (Kanazawa, Japan) and Iwate Medical University (Morioka, Japan).

### **Cell culture**

A human embryonic kidney-derived cell line HEK293 stably expressing UGT1A9 was previously established in my laboratory (Fujiwara et al., 2007b).

## **Preparation of monoclonal antibodies against UGT1A6, UGT1A8, UGT1A9, UGT1A10, UGT2B4, and UGT2B10**

The selection of antigenic peptide, peptide synthesis, and keyhole limpet hemocyanin conjugation were performed by Biogate (Gifu, Japan). Hydrophilicity, secondary structure, surface probability, and antigenicity were considered in the designation of the antigenic peptide sequence as follows: The hydrophilicity was evaluated by the method of Hopp and Woods (Hopp and Woods, 1981). The secondary structure was evaluated by the method of Chou-Fasman (Chou and Fasman, 1974) and the method of Robson (Garnier et al., 1978) using the GENETYX-MAC software (Software Development, Tokyo, Japan). The surface probability was evaluated by the method of Emini (Emini et al., 1985). Antigenicity was evaluated by the method of Welling (Welling et al., 1985) and the method of Parker (Parker et al., 1986) using original software. The designed peptide sequence was subjected to BLASTP search (<http://www.ncbi.nlm.nih.gov/blast/>) to screen its homology with known protein sequences. Based on these evaluations, sequences within the N-terminal half of each UGT isoforms were raised as candidate peptides (Table 1). At the N terminus of the synthesized peptides, a cysteine residue was added to facilitate conjugation to the carrier protein, keyhole limpet hemocyanin. The mouse monoclonal antibodies against the peptides were prepared by CLEA Japan (Tokyo, Japan) using a standard protocol. The hybridomas producing the antibodies were screened by ELISA with the synthesized peptide. Reactivity and specificity of antibody clones were evaluated by Western blotting as described below. A clone that specifically reacted with each UGT was expanded by intraperitoneal injection into mineral oil-primed mice. Monoclonal antibodies from mouse ascitic fluids were partially purified by precipitation with 33% ammonium sulfate.

**Table 1.** Sequence alignment of the candidate peptide of UGT1A6, UGT1A8, UGT1A9, UGT1A10, UGT2B4, and UGT2B10 as the antigens with the corresponding region of the other UGTs.

Isoform	Accession No.	Sequence
UGT1A1	P22309	<sup>84</sup> QREDVKESFVSLGHNVFEN--DSFLQRVIKTYKKIKKDSA <sub>121</sub>
UGT1A3	P35503	<sup>85</sup> TQDEFDRHVLGHTQLYFET--EHFLKFFRSMAMLNMSL <sub>122</sub>
UGT1A4	P22310	<sup>85</sup> TQKEFDRVTLGYTQGFET--EHLKRYRSMAIMNNVSL <sub>122</sub>
UGT1A5	P35504	<sup>85</sup> TQDEFDRLLLGHTQSFFET--EHLLMKFSRRMAIMNNMSL <sub>122</sub>
<b>UGT1A6</b>	P19224	<sup>83</sup> <b>DQEELKNRYQSF</b> GNNHFAE--RSFLTAPQTEYRNNMIVIG <sub>120</sub>
UGT1A7	NP_061950	<sup>82</sup> TLEDQDREFMVFADARWTAPLRSAFSLTSSSNG---IFD <sub>118</sub>
<b>UGT1A8</b>	AAB8425	<sup>82</sup> <b>TLEDLDREFMDFADAQWKAQVRS</b> LFSLFLSSSNG---FFN <sub>118</sub>
<b>UGT1A9</b>	NP_066307	<sup>82</sup> <b>TLEDLDREFKAF</b> AHAQWKAQVRSIYSLLMGSYND---IFD <sub>118</sub>
<b>UGT1A10</b>	AAB81537	<sup>82</sup> <b>TLEDQNR</b> EFMVF <sup>AHAQWKAQAQSIFSLLMSSSSG---FLD<sub>118</sub></sup>
<b>UGT2B4</b>	P06133	<sup>86</sup> <b>EFEDI</b> IKQLV <sup>KRWAEZLPKDT</sup> FWSYFSQVQEIMWTFN <sub>121</sub>
UGT2B7	P16662	<sup>86</sup> ELENFIMQOIKRWSZDLPKDTFWLYFSQVQEIMWTFN <sub>121</sub>
<b>UGT2B10</b>	P36537	<sup>84</sup> <b>EFENI</b> IMQLV <sup>KRLS-EIQKDT</sup> FWL <sup>PFSQEQE</sup> ILWAIN <sub>119</sub>
UGT2B11	AAC27891	<sup>86</sup> EFENIIMQOVKRWSDIRKDSFWLYFSQEQEILWELY <sub>120</sub>
UGT2B15	P54855	<sup>86</sup> YLEDSSLKILDRWIYGVSKNTFWSYFSQLQELCWEYY <sub>121</sub>
UGT2B17	AAC25491	<sup>86</sup> DLEDFFMKMFDRWTYSISKNTFWSYFSQLQELCWEYS <sub>121</sub>
UGT2B28	NP_444267	<sup>86</sup> EFENIIMQOVKRWSDIQKDSFWLYFSQEQEILWEFH <sub>120</sub>

The peptides used as antigens in this study are shown in bold letters.

## SDS-PAGE and Western blot analysis

For the analysis of UGTs, UGT Supersomes and microsomes from human, mouse, or rat tissues were separated by 10% SDS-polyacrylamide gel electrophoresis (PAGE) and transferred to Protran nitrocellulose membranes (Whatman GmbH, Dassel, Germany). The quantity of protein loaded onto gels was decided to be in the range showing linearity. In some cases, human liver microsomes or recombinant UGT1A9 proteins were treated with Endo H which cleaves the bond between two *N*-acetylglucosamines directly proximal to asparagine residue or PNGase F which cleaves the bond between asparagine and the *N*-acetylglucosamine residue. The enzyme sources were adjusted to a 2 mg/ml protein concentration with a denaturing buffer containing a final concentration of 0.5% SDS and 40 mM dithiothreitol and subsequently were denatured at 95°C for 10 min. An aliquot was incubated with 250 U of Endo H in 50 mM sodium citrate buffer (pH 5.5) or 500 U of PNGase F in 50 mM sodium phosphate buffer (pH 7.5) containing 1% NP-40 at 37°C for 1 h.

For the analysis of HNF1 $\alpha$ , 50  $\mu$ g of human liver homogenates were separated by 7.5%

SDS-PAGE and transferred to a polyvinylidene difluoride (PVDF) Immobilon-P membrane (Millipore, Billerica, MA). For the analysis of  $\beta$ -actin, 10  $\mu$ g of human liver microsomes or homogenates were separated by 7.5% SDS-PAGE and transferred to PVDF membranes.

After incubation in Odyssey blocking buffer (LI-COR Biosciences, Lincoln, NE) for 1 h, the membranes were probed with either 1:500 diluted anti-each UGT antibody, 1:200 diluted anti-HNF1 $\alpha$  antibody, or 1:200 diluted anti- $\beta$ -actin antibody for 3 h followed by incubation with the corresponding fluorescent dye-conjugated secondary antibodies. The UGTs or HNF1 $\alpha$  protein levels in individual human liver samples were normalized to  $\beta$ -actin protein levels. The band densities were quantified with the Odyssey Infrared Imaging system (LI-COR Biosciences).

### **Glucuronide formation assays**

Serotonin *O*-glucuronide formation was measured according to Krishnaswamy et al. (2003) with slight modifications. Briefly, a typical incubation mixture (100  $\mu$ l of total volume) contained 25 mM potassium phosphate buffer (pH 7.4), 2.5 mM MgCl<sub>2</sub>, 5 mM UDPGA, 25  $\mu$ g/ml alamethicin, 0.25 mg/ml microsomal preparation or UGT Supersomes, and 5 mM serotonin. The reactions were initiated by the addition of UDPGA and were then incubated at 37°C for 30 min. The reactions were terminated by addition of 100  $\mu$ l of acetonitrile. After removal of the protein by centrifugation at 13,000 g for 5 min, a 20- $\mu$ l portion of the sample was subjected to HPLC.

Propofol *O*-glucuronide formation was measured according to Fujiwara et al. (2007b) with slight modifications. Briefly, a typical incubation mixture (200  $\mu$ l of total volume) contained 50 mM potassium phosphate buffer (pH 7.4), 10 mM MgCl<sub>2</sub>, 3 mM UDPGA, 25  $\mu$ g/ml alamethicin, 0.5 mg/ml microsomal preparation or UGT Supersomes, and 500  $\mu$ M propofol. The reaction were initiated by addition of UDPGA and were then incubated at 37°C for 30 min. The reactions were terminated by addition of 200  $\mu$ l of acetonitrile. After removal of the protein by centrifugation at 13,000 g for 5 min, a 50- $\mu$ l portion of the sample was subjected to HPLC.

Nicotine *N*-glucuronide formation was measured according to Nakajima et al. (2002) with slight modifications. Briefly, a typical incubation mixture (200  $\mu$ l of total volume) contained 20 mM Tris-HCl buffer (pH 7.4), 5 mM MgCl<sub>2</sub>, 2.5 mM UDPGA, 25  $\mu$ g/ml alamethicin, 0.25 mg/ml microsomal preparation or UGT Supersomes, and 50  $\mu$ M nicotine. The reactions were initiated by addition of UDPGA and were then incubated at 37°C for 60 min. The reactions were terminated by boiling for 10 min. After removal of protein by centrifugation at 10,000 rpm for 5 min, a 9- $\mu$ l solution containing phosphoric acid and heptane sulfonate sodium to make the concentrations of these chemicals the same as those in the mobile phase. A 20- $\mu$ l portion of the sample was subjected to HPLC. The quantification of nicotine *N*-glucuronide was performed by comparing the HPLC peak height to that of the authentic standard. For the quantification of the other glucuronides, the eluate from the HPLC column containing each glucuronide was collected and a part of the eluate was hydrolyzed with NaOH at 75°C for 30 min (Hawes, 1998). The hydrolyzed glucuronides were quantified using HPLC by comparison of peak heights to those of external standard curve of the aglycones.

### **Statistical analyses**

Correlation analyses were performed by the Pearson's product-moment method. Differences between groups were determined by analysis of variance followed by the Tukey's multiple comparison test. A value of  $p < 0.05$  was considered statistically significant.

## **RESULTS**

### **Selection of peptide antigens to generate UGT1A6, UGT1A8, UGT1A9, UGT1A10, UGT2B4, and UGT2B10 antibodies**

Initially, preparation of a mouse monoclonal antibody against UGT1A9 was attempted using a histidine-tagged full-length UGT1A9 protein as an antigen. However, all of the resulting antibody clones (30 clones) cross-reacted with other UGT1A isoforms (data not shown). The full-length amino acid sequence of UGT1A9 exhibits homology with UGT1A7, UGT1A8, and UGT1A10 in excess of 89% (Table 2). Therefore, next the monoclonal

antibody was sought to be prepared using a UGT1A9 peptide as an antigen. Although peptides ranging from 10-20 amino acid residues in length are generally employed for antigens, a relatively longer peptide was employed expecting that it could recognize three-dimensional structure. Residues 87 to 118 of UGT1A9 (32 amino acids) were selected as an antigen (Table 1)—this peptide sequence is contained within the longer peptide antigen (82 amino acids, residues 61 to 142) used by Girard et al. (2004). The amino acid homology of the two different antigenic peptides with the corresponding residues of UGT1A7, UGT1A8, and UGT1A10 was 59-63% (32 residue peptide) versus 80% (82 residue peptide) (Table 2). Thus, the peptide comprising the 87 to 118 amino acid residues of UGT1A9 was used as an antigen. Each peptide of the other UGT isoforms, UGT1A6, UGT1A8, UGT1A10, UGT2B4, and UGT2B10 was also selected (Table 1). The amino acid homology of the selected antigenic peptides with the corresponding residues of the other peptides was 78% at the highest (Tables 2 and 3).

**Table 2.** Amino acid identities of antigenic peptides or full-length sequences within UGT1As.

UGT1A isoform	Amino acid identity (%)							
	UGT1A6		UGT1A8		UGT1A9		UGT1A10	
	Peptide	Full-length	Peptide	Full-length	Peptide	Full-length	Peptide	Full-length
UGT1A1	30	68	10	66	9	67	13	66
UGT1A3	18	67	7	67	6	67	13	66
UGT1A4	12	67	7	66	6	68	3	65
UGT1A5	12	68	7	68	13	68	7	66
UGT1A6	-	-	10	68	9	69	7	68
UGT1A7	6	68	72	94	59	93	69	90
UGT1A8	9	68	-	-	63	94	69	90
UGT1A9	9	69	69	94	-	-	66	89
UGT1A10	6	68	69	90	63	89	-	-

**Table 3.** Amino acid identities of antigenic peptides or full-length sequences within UGT2Bs.

UGT2B isoform	Amino acid identity (%)			
	UGT2B4		UGT2B10	
	Peptide	Full-length	Peptide	Full-length
UGT2B4	-	-	67	86
UGT2B7	67	86	58	88
UGT2B10	64	86	-	-
UGT2B11	58	86	75	91
UGT2B15	45	79	31	78
UGT2B17	45	78	39	77
UGT2B28	61	84	78	89

## Specificity of the prepared antibodies against each UGT isoform

The specificity of the candidate antibody clones was evaluated by Western blot analysis using a panel of recombinant human UGT1A or UGT2B isoforms. Fifteen out of 62 clones, 11 out of 48 clones, 5 out of 40 clones, 4 out of 60 clones, 8 out of 54 clones, and 4 out of 139 clones reacted with recombinant UGT1A6, UGT1A8, UGT1A9, UGT1A10, UGT2B4, and UGT2B10, respectively, without cross-reacting with the other UGT isoforms (data not shown). From them, each one clone exhibiting the highest reactivity for the corresponding UGT isoform was selected for expansion and antibody production. The specificity of the purified antibodies was then confirmed (Fig. 2).

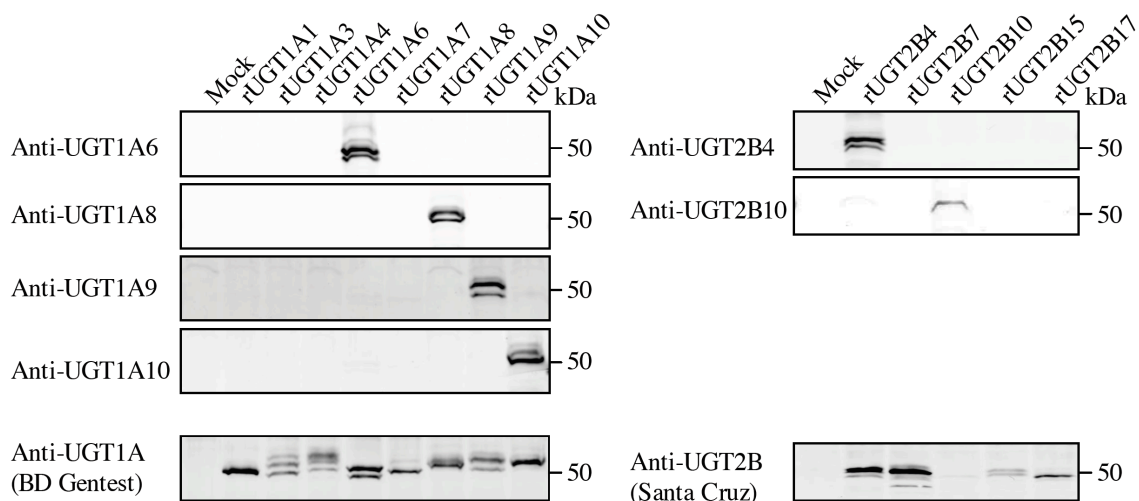


**Fig. 2.** Western blot analyses using the monoclonal antibodies against UGT1A6, UGT1A8, UGT1A9, UGT1A10, UGT2B4, and UGT2B10. Recombinant UGTs (1  $\mu$ g) expressed in baculovirus-infected cells (Supersomes) were subjected to 10% SDS-PAGE.

## Reactivity of the antibody toward glycosylated or deglycosylated UGT1A9

UGT1A9 is glycosylated at three asparagine residues at position 71, 292, and 344 (Nakajima et al., 2010). Three bands observed in UGT1A9 Supersomes (Fig. 2) would represent differently glycosylated species of UGT1A9, because none of them were observed in the control Supersomes. It was investigated whether the antibody could recognize both glycosylated and de- or un-glycosylated UGT1A9. When the UGT1A9 Supersomes were

treated with Endo H, the upper two bands observed in the non-treated sample disappeared, and a band with higher mobility was observed. The density of the faster migrating band appeared higher than that of the sum of the upper two bands (Fig. 3, left). The fastest migrating band in the non-treated sample might be glycosylated form that is tolerable to Endo H or other post-translationally modified form. The recombinant UGT1A9 stably expressed in HEK293 cells also showed three bands (Fig. 3, left), but the upper two bands would be non-specific bands because they were observed in homogenates from mock HEK293 cells too (data not shown). The difference in the band patterns between UGT1A9 Supersomes and UGT1A9 in HEK293 cells might reflect the differences in the extent of glycosylation and/or size of the glycan in insect or mammalian cells. When the recombinant UGT1A9 in HEK293 cells was treated with Endo H, the fastest migrating band was clearly shifted (Fig. 3, left). The band density was higher than that in the non-treated sample. As for HLM, the mobility of UGT1A9 was similar to that of UGT1A9 expressed in HEK293 cells, and UGT1A9 in HLM appeared to show some tolerance to Endo H. Next, PNGase F, which can cleave Endo H-resistant *N*-glycans (likely *N*-glycans from which two mannose subunits are removed by Golgi  $\alpha$ -mannosidase II) was used. By the treatment of HLM with PNGase F, only a band with faster mobility was observed, indicating that the upper band observed in Endo H-treated HLM would be the Endo H-resistant glycosylated UGT1A9 (Fig. 3, right). In the cases of UGT1A9 Supersomes and UGT1A9 in HEK293 cells, the results with PNGase F treatment were the same with those with Endo H treatment. It is interesting that the deglycosylated UGT1A9 in UGT1A9 Supersomes, UGT1A9 in HEK293, and HLM differently migrated, although it is still unclear that other post-translational modification such as phosphorylation may be involved. Taken together, these results suggest that the antibody can recognize UGT1A9 regardless of glycosylation status, although the reactivity seems to be enhanced for unglycosylated UGT1A9.

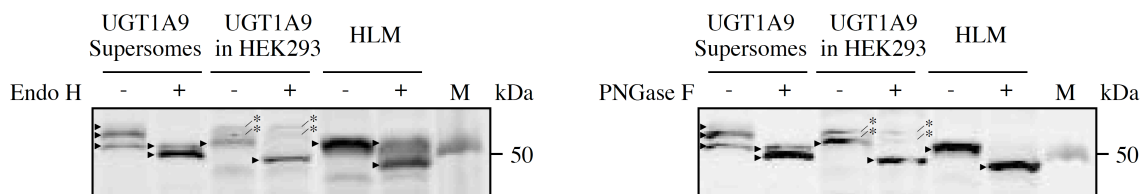


**Fig. 3.** Western blot analyses using the monoclonal antibody against human UGT1A9. Endo H (left panel) or PNGase F (right panel)-treated (+) and non-treated (-) UGT1A9 Supersomes (2.5  $\mu$ g), recombinant UGT1A9 stably expressed in HEK293 (40  $\mu$ g), and HLM (30  $\mu$ g) were subjected. The arrowhead and asterisk represent UGT1A9 and non-specific band, respectively. HLM, human liver microsomes; M, marker.

### UGT protein expression in microsomes from liver, kidney, and small intestine of human, rat, and mouse

Although previous studies revealed the expression profiles of UGT mRNA in human tissues (Nakamura et al., 2008; Ohno and Nakajin, 2009; Court et al., 2012), the expression profiles of UGTs at protein levels have not been fully clarified. Thus, microsomes from human liver, kidney, and small intestine were subjected to Western blot analysis (Fig. 4). Commercially available anti-UGT1A and anti-UGT2B antibodies non-specifically detected UGT1A and UGT2B isoforms, respectively, in the tissues. The expression levels were expressed relative to the value in recombinant expression system set at 100. UGT1A6 protein was highly expressed in the liver ( $7.0 \pm 0.4$  unit/ $\mu$ g, mean  $\pm$  SD) and kidney ( $6.7 \pm 0.1$ ), but negligible expression ( $0.6 \pm 0.1$ ) was observed in the small intestine. High expression of UGT1A9 protein was detected in the kidney ( $21.4 \pm 2.1$ ), followed by the liver ( $10.6 \pm 1.8$ ), but no expression was observed in the small intestine. UGT1A10 was detected only in the small intestine ( $1.8 \pm 0.3$ ). UGT2B4 ( $27.6 \pm 2.3$ ) and UGT2B10 ( $105.2 \pm 1.1$ ) were detected only in the liver. UGT1A8 was detected in the liver ( $5.6 \pm 0.1$ ) and to a lesser extent kidney ( $1.3 \pm 0.2$ ) as well as small intestine ( $6.0 \pm 0.4$ ). These protein expression profiles were largely consistent with the previously reported mRNA expression profiles except UGT1A8 detected in the liver and kidney (Ohno and Nakajin, 2009; Court et al., 2012).

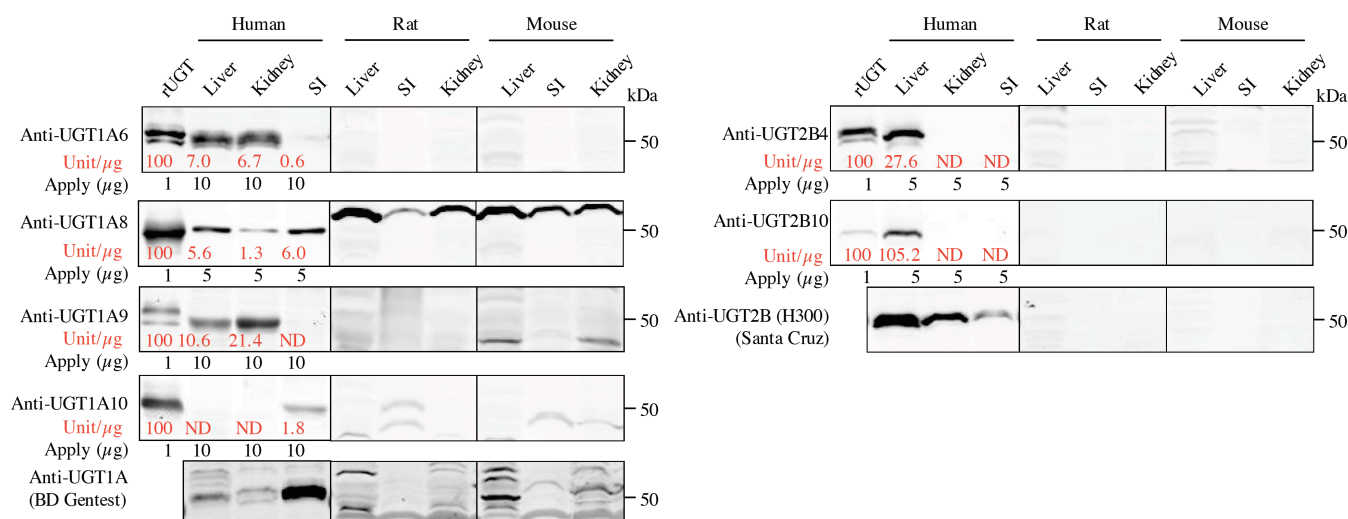


**Fig. 4.** Western blot analyses of tissue microsomes from human, rat, and mouse using the monoclonal antibodies against UGT1A6, UGT1A8, UGT1A9, UGT1A10, UGT2B4, and UGT2B10. Tissue microsomes were subjected to 10% SDS-PAGE. UGT expression levels (unit/ $\mu$ g) are the mean of triplicate determinations. rUGT: recombinant UGT Supersomes; ND: not detected; SI: small intestine.

Next, reactivity of the antibodies toward Ugts in mouse and rat liver, small intestine, and kidney microsomes was examined. As shown in Fig. 4, no clear band was detected in rat and mouse tissue microsomes, suggesting that the antibody does not react with any Ugt in mouse and rat tissues microsomes.

### Normalized activities of UGT1A6, UGT1A9, and UGT2B10 in recombinant systems and human tissue microsomes

The UGT protein expression levels determined with the prepared antibodies enabled to know normalized activities per unit of each UGT. The serotonin *O*-glucuronidation activities in recombinant UGT, HLM, HKM, and HIM were  $2,744 \pm 38$ ,  $10,149 \pm 465$ ,  $6,874 \pm 745$ , and  $706 \pm 34$  pmol/min/mg protein, respectively (Fig. 5A). The propofol *O*-glucuronidation activities in these enzyme sources were  $3,849 \pm 176$ ,  $3,136 \pm 378$ ,  $8,386 \pm 170$ , and  $4,020 \pm 1,162$  pmol/min/mg protein, respectively (Fig. 5A). The nicotine *N*-glucuronidation activities in recombinant UGT2B10 and HLM were  $0.92 \pm 0.81$  and  $22.40 \pm 1.42$  pmol/min/mg protein, respectively, and was not detected in HKM and HIM (Fig. 5A). These enzyme activities were normalized to the corresponding UGT protein expression level (Fig. 5B). The normalized serotonin *O*-glucuronidation activity per unit of UGT in UGT1A6 Supersomes was 37- to

52-fold lower than those in human tissue microsomes (Fig. 5B). The normalized propofol *O*-glucuronidation activity per unit of UGT in UGT1A9 Supersomes was 8- to 10- fold lower than those in human tissue microsomes (Fig. 5B). The normalized nicotine *N*-glucuronidation activity per unit of UGT in UGT2B10 Supersomes was 19-fold lower than that in human liver microsomes (Fig. 5B). Thus, it was demonstrated that the normalized activities per unit of each UGT in UGT Supersomes were remarkably lower than those in human tissue microsomes.

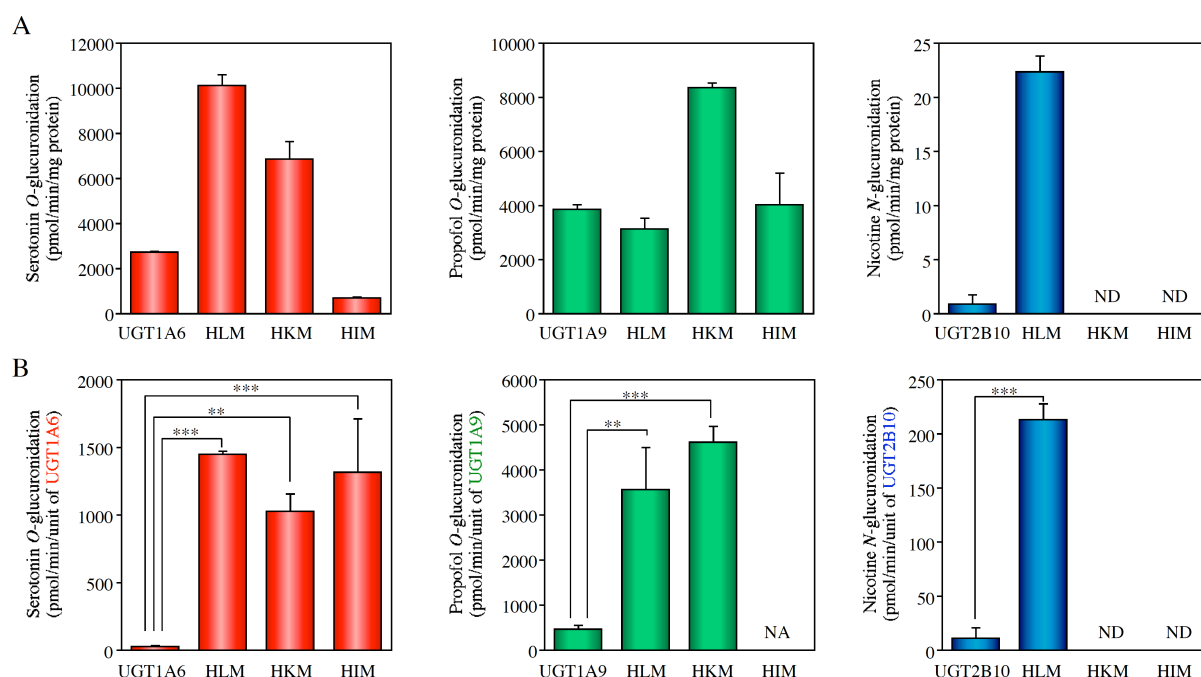


**Fig. 5.** Serotonin *O*-, propofol *O*-, and nicotine *N*-glucuronidations in recombinant UGT and human tissue microsomes. The activities were expressed as pmol/min/mg protein (A) and pmol/min/unit of UGT (B). Each column represent mean  $\pm$  SD (n = 3). \*\* $p$  < 0.01 and \*\*\* $p$  < 0.001. ND: not detected; NA: not applicable.

### Expression levels of UGT1A6, UGT1A9, UGT2B4, and UGT2B10 protein in individual human livers and the correlation of protein levels with mRNA levels and enzymatic activities

The relative expression levels of UGT1A6, UGT1A9, UGT2B4, and UGT2B10 protein in a panel of 20 human liver microsomes were determined (Fig. 6A). The interindividual variabilities of UGT1A6, UGT1A9, UGT2B4, and UGT2B10 were 10-, 9-, 6-, and 7-fold, respectively (Fig. 6A). The UGT1A6, UGT1A9, and UGT2B10 protein levels were correlated with serotonin *O*-glucuronidation ( $r = 0.82$ ,  $p < 0.0001$ ), propofol *O*-glucuronidation ( $r = 0.48$ ,

$p < 0.05$ ), and nicotine *N*-glucuronidation ( $r = 0.61$ ,  $p < 0.01$ ), respectively (Fig. 6B).

However, their protein levels besides those of UGT2B4 were not correlated with the corresponding mRNA levels that were determined in the previous study (Fig. 6C) (Izukawa et al., 2009). UGT2B4 protein levels also were not correlated with its mRNA levels.

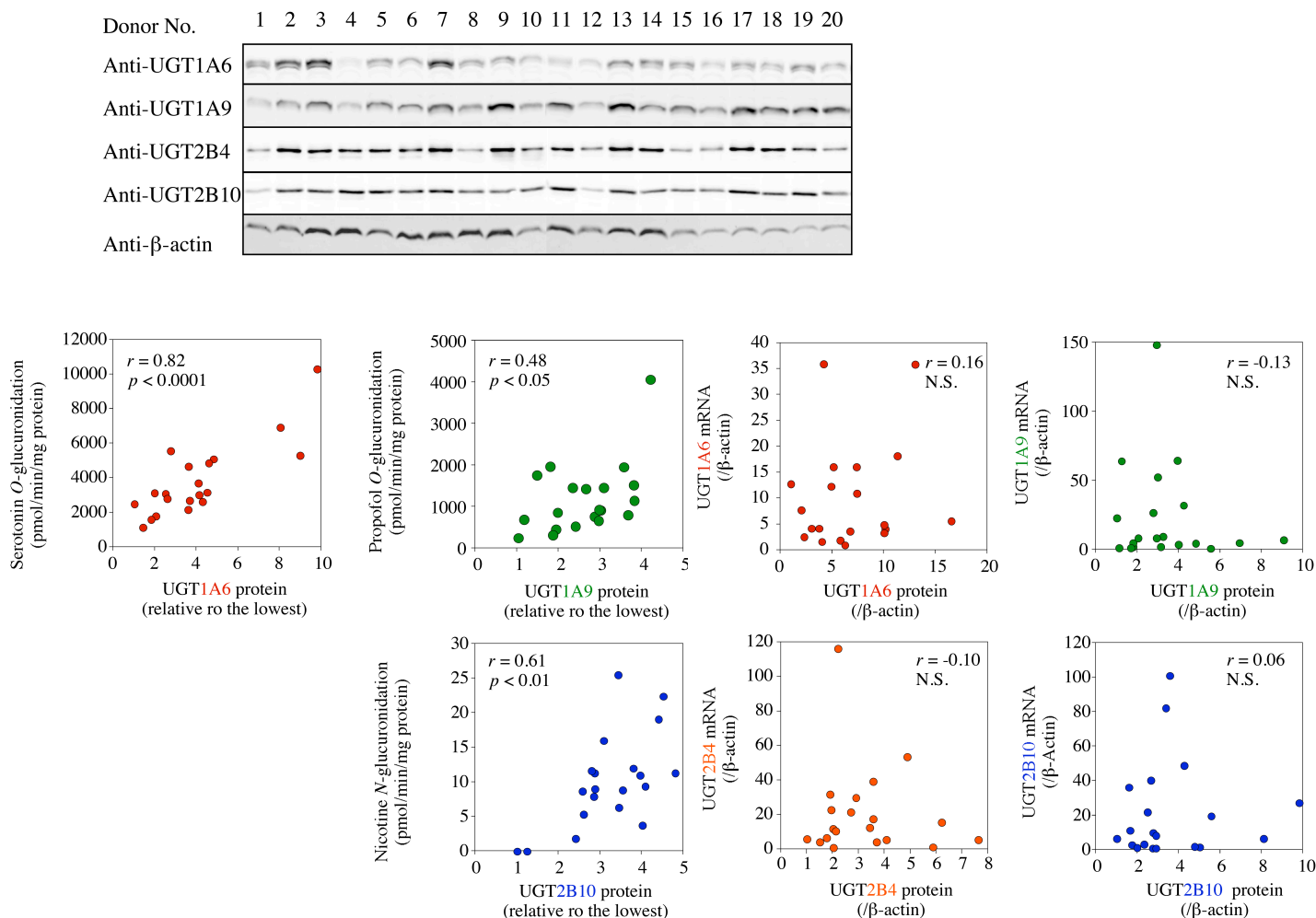


**Fig. 6.** Interindividual variability of UGT protein levels in human liver and its correlation with enzyme activity, UGT1A9 mRNA or HNF1 $\alpha$  protein levels. (A) The expression levels of UGT1A6, -1A9, -2B4, and -2B10 proteins in 20 human liver microsomes were determined by Western blot analysis. Data are representative of two experiments. Relationships (B) between UGT protein levels and serotonin *O*-glucuronosyltransferase activities, propofol *O*-glucuronosyltransferase activities, or nicotine *N*-glucuronosyltransferase activities, and (C) between UGT protein levels and UGT mRNA levels were analyzed. The serotonin *O*-, propofol *O*-, and nicotine *N*-glucuronosyltransferase activities were measured at a substrate concentration of 5000, 500, and 50  $\mu$ M, respectively. The UGT mRNA levels were normalized to  $\beta$ -actin mRNA levels. The UGT protein levels were normalized to  $\beta$ -actin protein levels. The values represent the levels relative to that of the lowest sample. Each data point is the mean of duplicate experiments. N.S. not significant.

## Relationship between HNF1 $\alpha$ protein levels and UGT protein or mRNA levels in individual human livers

Previous studies reported that HNF1 $\alpha$  and HNF4 $\alpha$  mRNA levels were strongly correlated with UGT1A6 and UGT1A9 mRNA levels in a panel of human livers (Aueviriyavit et al., 2007; Ramírez et al., 2008). This is consistent with the finding that HNF1 $\alpha$  and HNF4 $\alpha$  contribute to the regulation of UGT1A9 (Barbier et al., 2005; Gardner-Stephen and Mackenzie, 2007). In addition, potential binding sites for HNF1 $\alpha$  and HNF4 $\alpha$  have been identified in the proximal promoter of most known UGTs (Gardner-Stephen et al., 2005). However, the HNF protein levels rather than mRNA level should be considered. Thus, the relationship between the HNF1 $\alpha$  protein levels and the UGT protein or mRNA levels was examined. As the results, it was demonstrated that the HNF1 $\alpha$  protein levels were significantly correlated with the UGT1A6 ( $r = 0.49, p < 0.05$ ) and UGT1A9 mRNA levels ( $r = 0.52, p < 0.05$ ), but not with UGT2B4 and UGT2B10 mRNA levels (Fig. 7A). In contrast, neither UGT protein levels were correlated with the HNF1 $\alpha$  protein levels (Fig. 7B). These data suggest that while HNF1 $\alpha$  would regulate UGT1A6 and UGT1A9 at the transcriptional level, their protein levels are being regulated at the post-transcriptional level.

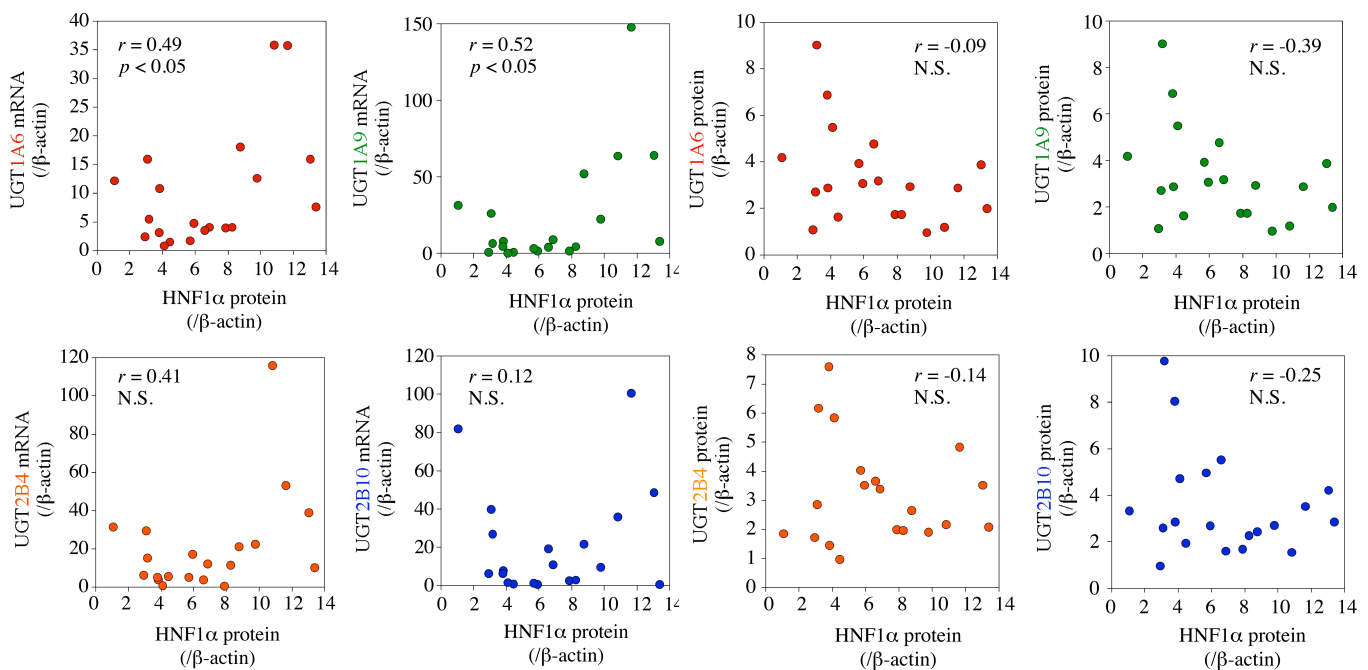


**Fig. 7.** Correlation analyses between HNF1 $\alpha$  protein levels and UGT mRNA or protein levels in a panel of 20 human livers. Relationships (A) between HNF1 $\alpha$  protein levels and UGT mRNA levels, and (B) between HNF1 $\alpha$  protein levels and UGT protein levels were analyzed. The UGT mRNA levels were normalized to  $\beta$ -actin mRNA levels were analyzed. The UGT and HNF1 $\alpha$  protein levels were normalized to  $\beta$ -actin protein levels. The values represent the levels relative to that of the lowest sample. Each data point is the mean of duplicate experiments. N.S. not significant.

## DISCUSSION

Among the 19 human UGT isoforms, UGT1A1, UGT1A3, UGT1A4, UGT1A6, UGT1A9, UGT2B7, and UGT2B15 are the isoforms of greatest importance in hepatic drug elimination, although pre-hepatic glucuronidation by UGT1A7, UGT1A8, and UGT1A10 may additionally influence bioavailability (Miners et al., 2006). In addition to them, hepatic UGT2B10 was recently found to show high affinity for clinically important drugs (Kato et al., 2013). There is now accumulating evidence for the expression profiles of UGTs in human tissues at mRNA level (Nakamura et al., 2008; Ohno and Nakajin, 2009; Court et al., 2012). However, information regarding their protein has been limited by the lack of isoform-specific antibodies. Although there were previous attempts to generate specific antibodies against UGT1A9 (Ikushiro et al., 2006; Girard et al., 2004), the antibodies recognized other UGT1A isoforms such as UGT1A6 (Ikushiro et al., 2006), UGT1A7, UGT1A8, and UGT1A10 (Girard et al., 2004). Furthermore, when we evaluated the specificity of commercially available antibodies against UGT1A9 (Abcam, Cambridge, UK and Abnova, Taipei, Taiwan), it was observed that these antibodies cross-reacted with other UGT1A isoforms (unpublished data). Although an antibody against UGT2B4 was prepared (Pillot et al., 1993), the specificity was not evaluated. Based on the background, this study was performed to prepare specific antibodies against each human UGT and succeeded in generation of antibodies that specifically recognize UGT1A6, UGT1A8, UGT1A9, UGT1A10, UGT2B4, and UGT2B10.

Upon Western blotting using the prepared antibodies, there were no aggregated UGTs at the interface between upper and lower gels or the bottom of the wells in any enzyme source (data not shown). It was confirmed that these antibodies did not cross-react with the other human UGT isoforms. The tissue distribution of UGT1A6, UGT1A9, UGT1A10, UGT2B4, and UGT2B10 protein was largely consistent with previously reported mRNA data (Nakamura et al., 2008; Ohno and Nakajin, 2009). Unexpectedly, UGT1A8 protein was detected in the liver and kidney as well as small intestine, which was inconsistent with the mRNA expression showing the exclusive expression in the gastrointestinal tract but not in the liver and kidney (Ohno and Nakajin, 2009; Court et al., 2012). It was surmised that the

prepared antibody against UGT1A8 non-specifically reacted with proteins other than UGTs in human tissues.

It was interesting that the expression of UGT1A9 protein was higher in the kidney than that in liver (Fig. 4). Although the kidney plays a role in the excretion of polar xenobiotics and metabolites, increasing evidence reveals that the kidney significantly contributes to metabolic clearance of therapeutic drugs, such as non-steroidal anti-inflammatory drugs, propofol, and mycophenolic acid, and to the maintenance of renal homeostasis through inactivating mediators, such as prostaglandins, leukotrienes, epoxyeicosatrienoic acids, and hydroxyeicosatetraenoic acids (Knights and Miners, 2010). Because these drugs or endobiotics are known to be substrates of UGT1A9 (Knights and Miners, 2010), it has been speculated that UGT1A9 would contribute to their clearance. There has been only one report of the immunohistochemical detection of UGT1A in kidney (Gaganis et al., 2007), although the precise isoforms detected remain unknown. The present study supports the role of UGT1A9 in the kidney, as indicated by the substantial expression of UGT1A9 protein detected by Western blotting. The antibodies that were prepared in the present study will be useful for future immunohistochemical studies of UGTs.

An interesting finding using the prepared antibodies was that the normalized activities of UGT1A6, UGT1A9, and UGT2B10 in recombinant systems were unambiguously lower than those in human tissue microsomes (Fig. 5). This might be attributable to the differences in membrane circumstance including lipid components and/or post-translational modification between recombinant systems and human tissue microsomes. Another possible explanation is the presence of other UGT isoforms in human tissue microsomes. Previous studies (Fujiwara et al., 2007a, 2007b, and 2010) demonstrated that the co-expression of another UGT isoform increases the UGT1A6-catalyzed serotonin *O*-glucuronidation and UGT1A9-catalyzed propofol *O*-glucuronidation in HEK293 cells. Apart from these reasons, it is notable that the activities of recombinant UGTs do not directly and quantitatively mirror the actual UGT activities in human tissues. In this regard, the relative activity factor approach (Crespi and Miller, 1999), which uses the ratio of activity of tissue microsomes and recombinant enzymes,

would be useful to estimate the contributions of individual UGTs to a given metabolic pathway in tissue microsomes, as recent studies reported (Kato et al., 2012; Zhu et al., 2012).

Moderate interindividual variability (6- to 10-fold) was found in the hepatic UGT1A6, UGT1A9, UGT2B4, and UGT2B10 expression at the protein level (Fig. 6). Several studies have sought to uncover the underlying mechanisms of the variability in the UGT expression, with particular focus on *cis*- or *trans*-acting factors. As *cis*-acting factors, genetic polymorphisms can be raised. The -275 *T>A* and -2152 *C>T* alleles, which are linked to each other, have been shown to be associated with higher hepatic UGT1A9 protein expression and increased rates of propofol and mycophenolic acid glucuronidation (Girard et al., 2004). In addition, homozygotes for the intronic SNP at position *IVS1+399C>T* have been shown to exhibit higher (1.3 fold) hepatic UGT1A9 protein levels (Girard et al., 2006). In these studies, UGT1A9 protein was assessed using the UGT1A7-10 antibody. The fact that UGT1A7, UGT1A8, and UGT1A10 are not expressed in liver made such studies possible. In contrast, antibodies prepared in this study would be applicable for the evaluation of the effects of this SNP on UGT1A9 expression in extrahepatic tissues expressing UGT1A9 and the closely related isoforms UGTs 1A7, 8, and 10, such as kidney and adrenal tissues (Ohno and Nakajin, 2009). For the *UGT1A6* gene, although several polymorphisms were identified in the 5'-regulatory region, there were no associations between the polymorphisms and UGT1A6 expression levels in a panel of human 54 livers (Krishnaswamy et al., 2005). Transcription factors might be another factor determining the variability of UGT expression. It has been reported that HNF1 $\alpha$  and HNF4 $\alpha$  positively regulate the expression of UGT1A9 (Barbier et al., 2005; Gardner-Stephen and Mackenzie, 2007). A significant positive correlation between these factors and UGT1A6 or UGT1A9 at the mRNA level in human livers has been reported (Aueviriyavit et al., 2007; Ramírez et al., 2008). Beyond these reports, this study demonstrated that HNF1 $\alpha$  protein levels are significantly correlated with UGT1A6 or UGT1A9 mRNA levels (Fig. 7). However, HNF1 $\alpha$  protein levels were not correlated with UGT1A6 or UGT1A9 protein levels (Fig. 7), as any correlation was not observed between mRNA and protein levels of UGT1A6 or UGT1A9 (Fig. 6). Lack of correlation between the

mRNA and protein levels was also observed with other UGTs, such as UGT2B4, UGT2B10 (Fig. 6), UGT1A4 and UGT2B7 in the present and previous studies (Izukawa et al., 2009). Therefore, it is reasonable to speculate that post-transcriptional and/or post-translational regulation plays a role in UGT protein levels. MicroRNAs (miRNAs) have recently received considerable attention as a critical factor of post-transcriptional regulation. My laboratory have reported that some cytochrome P450 isoforms and transcription factors, such as pregnane X receptor, vitamin D receptor, and HNF4 $\alpha$  are regulated by miRNAs (Nakajima and Yokoi, 2011), implicating a role of miRNA in clearance of drugs and endobiotics. It would be of interest to investigate whether miRNAs may be involved in the regulation of UGTs. Generally mammalian miRNAs bind to the 3'-untranslated region (3'-UTR) of the target mRNA to cause translational repression or mRNA degradation. Because the 3'-UTR sequences of UGT1As are common, it is possible that UGT1As may be commonly regulated by the same miRNA.

The UGT1A9 protein levels in a panel of 20 individual human livers were moderately ( $r = 0.48, p < 0.05$ ) correlated with propofol glucuronidation (Fig. 6). The moderate correlation was consistent ( $r = 0.5, p < 0.0001, n = 48$ ) with the results reported by Girard et al. (2004). Because it was previously demonstrated that UGT enzyme activity could be modulated through formation of heterodimers with other UGT isoform (Fujiwara et al., 2007a and 2007b), such modulation might account for the moderate correlation. The prepared antibodies in this study might be useful tool to for studying heterodimers of UGTs.

In summary, specific monoclonal antibodies against human UGT1A6, UGT1A8, UGT1A9, UGT1A10, UGT2B4, and UGT2B10 were generated in this study. By Western blot analysis using these antibodies, it was demonstrated that human UGT proteins showed tissue-specific expression, supporting previous findings at mRNA levels. These antibodies can be used to assess tissue distribution and interindividual variability of UGT protein expression, and such evaluation may promote the understanding of physiological, pharmacological and toxicological role of UGTs.

## CHAPTER 3

### **Epigenetic regulation is a crucial factor in the repression of UGT1A1 expression in the human kidney**

#### **ABSTRACT**

Human UGT1A1 catalyzes the metabolism of numerous clinically and pharmacologically important compounds such as bilirubin and SN-38. UGT1A1 is predominantly expressed in the liver and intestine, but not in the kidney. The purpose of this study was to uncover the mechanism of the tissue-specific expression of UGT1A1, focusing on its epigenetic regulation. Bisulfite sequence analysis revealed that the CpG-rich region near the human *UGT1A1* promoter (-85 to +40) was hypermethylated (83%) in the kidney, whereas it was hypomethylated (24%) in the hepatocytes. A chromatin immunoprecipitation assay demonstrated that histone H3 near the promoter was hypoacetylated in the kidney but was hyperacetylated in the liver; this hyperacetylation was accompanied by the recruitment of HNF1 $\alpha$  to the promoter. The *UGT1A1* promoter in human kidney-derived HK-2 cells that do not express UGT1A1 was fully methylated, but was relatively unmethylated in human liver-derived HuH-7 cells that express UGT1A1. Treatment with 5-aza-2'-deoxycytidine (5-Aza-dC), an inhibitor of DNA methylation, resulted in an increase of UGT1A1 mRNA expression in both cell types, but the increase was much larger in HK-2 cells than in HuH-7 cells. The transfection of an HNF1 $\alpha$  expression plasmid into the HK-2 cells resulted in an increase of UGT1A1 mRNA only in the presence of 5-Aza-dC. In summary, this study demonstrated that DNA hypermethylation along with histone hypoacetylation interferes with the binding of HNF1 $\alpha$ , resulting in the defective expression of UGT1A1 in the human kidney. Thus, epigenetic regulation is a crucial determinant of tissue-specific expression of UGT1A1.

## INTRODUCTION

Human UGTs show tissue-specific expression. Although most UGTs are predominantly expressed in the liver, UGT1A7, UGT1A8, and UGT1A10 are exclusively expressed in the gastrointestinal tract (Strassburg et al., 1997 and 1998b). UGT1A1 is expressed in the liver, small intestine and colon, but not in the kidney (Nakamura et al., 2008; Ohno and Nakajin, 2009; Court et al., 2012). The expression of UGT2A1 and 2A2 are limited to the olfactory epithelium (Court et al., 2012). UGT2B7 is abundantly expressed in the liver, kidney, small intestine, and colon, whereas UGT2B10 is expressed only in the liver (Court et al., 2012). To understand the underlying mechanisms of the tissue-specific expression of UGTs, some studies were conducted with a focus on transcriptional regulation (Gardner-Stephen and Mackenzie, 2008; Mackenzie et al., 2010). It has been demonstrated that the intestine-specific transcription factor, Cdx2, Sp1 and HNF1 $\alpha$  regulate UGT1A8 and 1A10 expression in the intestine (Gregory et al., 2003, 2004a, and 2004b). HNF1 $\alpha$  and Cdx2 cooperatively regulate UGT2B7 expression in the intestine, whereas HNF1 $\alpha$  and octamer transcription factor-1 cooperatively regulate its expression in the liver and kidney (Gregory et al., 2006). HNF1 $\alpha$  is also involved in the regulation of UGT1A1 expression in the liver (Bernard et al., 1999). Thus, knowledge of the transcriptional regulation of the tissue-specific expression of the UGTs is accumulating.

However, a question that has yet to be answered is why UGT1A1 is not expressed in the kidney, even though HNF1 $\alpha$  is expressed in this tissue (Rey-Campos et al., 1991). This study was performed to clarify the mechanisms underlying the defective expression of UGT1A1, with a focus on epigenetic regulation. It is known that epigenetic changes including DNA methylation and histone modification are key regulators of tissue-dependent gene expression (Shiota, 2004; Ohgane et al., 2008). Supporting this hypothesis, a previous study found that the DNA methylation status of the proximal promoter region of the *UGT1A1* gene affects UGT1A1 expression in colon cancer cell lines (Gagnon et al., 2006). In this study, DNA methylation and histone modification of human UGT1A1 in human liver and kidney were investigated.

## **MATERIALS AND METHODS**

### **Chemicals and reagents**

5-Aza-2'-deoxycytidine (5-Aza-dC) and trichostatin A (TSA) were purchased from Sigma-Aldrich. Goat anti-human HNF1 $\alpha$  polyclonal antibody (C-19), mouse anti- $\beta$ -actin monoclonal antibody (C-14), and control rabbit and goat IgGs were purchased from Santa Cruz Biotechnology. Rabbit anti-human acetyl histone H3 polyclonal antibody was purchased from Millipore. Primers were commercially synthesized at Hokkaido System Science (Sapporo, Japan). All other chemicals and solvents were of the highest grade commercially available.

### **Human tissues**

Human liver and kidney samples from five Japanese donors (donor 1, an 80-year-old female; donor 2, a 54-year-old male; donor 3, a 39-year-old female; donor 4, a 13-year-old male; donor 5, a 40-year-old male) were obtained from autopsy materials that were discarded after pathological investigation. The use of the human livers and kidneys was approved by the Ethics Committees of Kanazawa University (Kanazawa, Japan) and Iwate Medical University (Morioka, Japan).

### **Cell culture**

Human kidney tubular epithelial cell line HK-2 and human hepatocellular carcinoma cell line HuH-7 were obtained from the American Type Culture Collection (Manassas, VA) and the RIKEN BioResource Center (Ibaraki, Japan), respectively. These cells were cultured as previously described (Nakamura et al., 2008).

### **RNA isolation and real-time reverse transcription (RT)-polymerase chain reaction (PCR)**

Total RNA was isolated from human liver and kidney samples using RNAiso (Takara Bio, Otsu, Japan) according to the manufacturer's protocol. The cDNA was synthesized from the

total RNA using ReverTraAce (Toyobo, Osaka, Japan). The UGT1A1 mRNA levels were determined by real-time RT-PCR and normalized to glyceraldehyde-3-phosphate dehydrogenase (GAPDH) mRNA levels as described previously (Izukawa et al., 2009).

### Genomic DNA extraction and bisulfite reaction

Genomic DNA samples were prepared from human liver (donor 3) and kidney (donor 1) samples, cell lines, or human hepatocytes (HH268, a 54-year-old Caucasian female, Tissue Transformation Technologies, Edison, NJ) with a Genra Puregene Tissue kit (Qiagen, Valencia, CA). Five hundred nanograms of genomic DNA digested with *EcoR* I was treated with bisulfite using the EZ DNA Methylation kit (Zymo Research, Orange, CA). The DNA fragment near the transcription start site (TSS) of the *UGT1A1* gene was amplified by PCR using the primer pair shown in Table 4. The PCR products were cloned into the pT7Blue T-Vector (Novagen, Madison, WI), and randomly picked clones were sequenced. The DNA methylation status of the sequence was analyzed using the web-based tool QUMA (Kumaki et al., 2008).

**Table 4.** Oligonucleotides used for the UGT1A1 bisulfite analysis and ChIP assay and for the cloning of HNF1 $\alpha$ .

Oligonucleotides	5' to 3' sequence	Position
Bisulfite analysis of UGT1A1		
Forward	TTTGTGGATTGATAGTTTTTATAG	-113 to -89
Reverse	CAATAACTACCATCCACTAAAATC	+134 to +111
ChIP assay of UGT1A1		
Forward	CTACCTTTGTGGACTGACAGC	-118 to -98
Reverse	CAACAGTATCTTCCCAGCATG	+111 to +91
Cloning of HNF1 $\alpha$		
Forward	GCAGCCGAGCCATGGTTTCT	-11 to +9
Reverse	GGTGCCGTGGTTACTGGGA	+1906 to +1888

Nucleotides are numbered with the TSS designated as +1 in the UGT1A1 genomic DNA sequence and base A in the initiation codon ATG designated as +1 in the HNF1 $\alpha$  cDNA sequence.

### **Chromatin immunoprecipitation (ChIP) assay**

The ChIP assay was performed using the ChIP assay kit (Millipore) with slight modifications. Approximately 200 mg of frozen human liver (donor 3) or kidney (donor 1) was minced on ice and suspended in 1% (v/v) formaldehyde to cross-link proteins to DNA. After centrifugation, the precipitate was resuspended in cell lysis buffer and homogenized using a Dounce homogenizer. After centrifugation, the precipitate was resuspended in nuclei lysis buffer and sonicated to shear the genomic DNA. After centrifugation, the supernatant (100  $\mu$ L) was diluted ten-fold with IP dilution buffer and incubated with Dynabeads protein G (Life Technologies, Gaithersburg, MD) conjugated to antibodies against acetylated histone H3 (5  $\mu$ g) or HNF1 $\alpha$  (2  $\mu$ g). A proportion of the diluted supernatant was kept as an input. The Dynabeads protein G was precipitated and was washed sequentially one time each with a low-salt immune complex wash buffer, a high-salt immune complex buffer, and a LiCl immune complex buffer. The DNA-protein complex was eluted with elution buffer twice, and the cross-links were reversed by adding NaCl. DNA was extracted by phenol-chloroform extraction and ethanol precipitation. The -118 to +91 region of the *UGT1A1* gene was amplified by real-time PCR with the primers shown in Table 4. The protocol for the PCR was as follows: 95°C for 30 s followed by 45 cycles of 94°C for 4 s and 62°C for 20 s. DNA extraction and real-time PCR were also performed for the input samples, and the data were used as a control to evaluate the enrichment of DNA in the immunoprecipitates.

### **Construction of an HNF1 $\alpha$ expression plasmid**

Human HNF1 $\alpha$  cDNA was amplified by PCR using the primer pair shown in Table 4 and human liver cDNA as a template. The PCR product was subcloned into the pTARGET vector (Promega, Madison, MI). The nucleotide sequence was confirmed by DNA sequencing analysis.

### **Chemical treatment and transfection of expression plasmid into the cells**

HK-2 and HuH-7 cells were seeded onto a 12-well plate at  $0.5 \times 10^5$  cells/well and

incubated for 24 h. For dose response experiments, the cells were treated with 0.01, 0.1, 1 or 10  $\mu\text{M}$  5-Aza-dC for 120 h or treated with 50, 100, or 300 nM TSA for 24 h and then subjected to RNA isolation. For the overexpression of HNF1 $\alpha$ , the cells were transiently transfected with 0.5  $\mu\text{g}$  of an HNF1 $\alpha$  expression plasmid or an empty pTARGET plasmid using the X-tremeGENE HP DNA transfection reagent (Roche Applied Science, Indianapolis, IN). After 12 h, the cells were treated with 0.1  $\mu\text{M}$  5-Aza-dC for 96 h, followed by treatment with TSA for an additional 24 h. The UGT1A1 mRNA levels were determined as described above.

### **Preparation of nuclear extract and immunoblot analysis of HNF1 $\alpha$**

Nuclear extract was prepared from HK-2 and HuH-7 cells transfected with the HNF1 $\alpha$  expression plasmid or empty plasmid using NE-PER Nuclear and Cytoplasmic extraction reagents (Thermo Fisher Scientific, Rockford, IL) according to the manufacturer's protocols. The protein concentration was determined using Bradford protein assay reagent (Bio-Rad Laboratories, Hercules, CA) with  $\gamma$ -globulin as a standard. The nuclear extract (40  $\mu\text{g}$ ) was separated by 7.5% SDS-PAGE and transferred to an Immobilon-P transfer membrane (Millipore). The membranes were probed with goat anti-human HNF1 $\alpha$  or rabbit anti-human GAPDH antibodies followed by fluorescent dye-conjugated second antibodies. The membranes were then scanned using the Odyssey Infrared Imaging system.

### **Statistical analyses**

For DNA methylation status, the statistical significance was evaluated by the Mann-Whitney *U*-test or Fisher's exact test using the web-based tool QUMA. For mRNA expression, statistical significance was determined using an unpaired, two-tailed Student's *t* test or one-way analysis of variance followed by Dunnett's test. When the *p* value was less than 0.05, the differences were considered to be statistically significant.

## RESULT

### UGT1A1 mRNA expression in human liver and kidney

UGT1A1 mRNA expression in human liver and kidney was determined by real-time RT-PCR. As shown in Fig. 8, UGT1A1 mRNA was detected in the liver, but was negligible in the kidney. The results supported previous studies (Nakamura et al., 2008; Ohno and Nakajin, 2009) that reported the repressed expression of UGT1A1 in the human kidney.

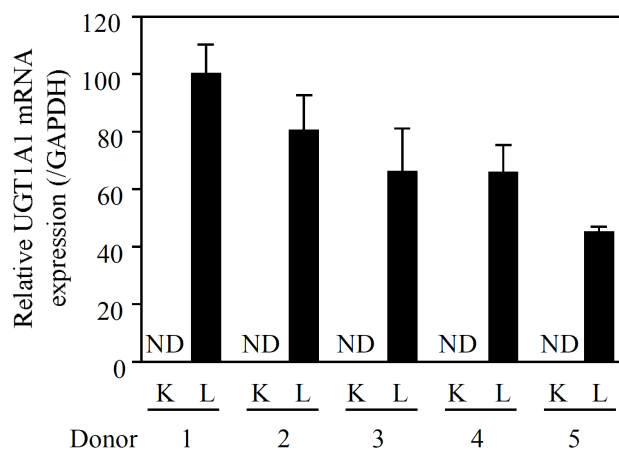


**Fig. 8.** UGT1A1 mRNA expression in human kidney and liver. The expression levels of UGT1A1 mRNA were determined by real-time RT-PCR and normalized to GAPDH mRNA levels. Each kidney and liver sample with a given number of donors came from the same donors. The values are expressed as relative to the UGT1A1 levels in the liver from donor 1. Each column represents the mean  $\pm$  SD of triplicate determinations. K, kidney; L, liver; ND, not detectable.

### DNA methylation status of the *UGT1A1* promoter region in human liver and kidney

Genomic DNA extracted from the liver and kidney was treated with bisulfite, and the promoter region of *UGT1A1* spanning -113 to +111 was amplified by PCR. The PCR product was subcloned into a vector, and 14 clones from each sample were sequenced. The DNA methylation status of the CpG dinucleotides at -85, -54, -12, +12, +36, and +40 of the *UGT1A1* gene is shown in Fig. 9. In the liver, 31 out of 84 CpG sites (37%) were methylated, whereas in the kidney, 70 out of 84 CpGs (83%) were methylated ( $p = 0.07$ , Mann-Whitney  $U$ -test). Notably, the methylated CpG sites were biased in five clones in the liver. It was surmised that these clones might be from hepatic nonparenchymal cells. Hence, the *UGT1A1* promoter in human hepatocytes was investigated and only 20 out of 84 CpG sites (24%) were found to be methylated. In particular, nucleotide positions -85, -54, and -12 were unmethylated in all hepatocyte clones, but were hypermethylated in the kidney ( $p < 0.001$ ,  $p < 0.01$ , and  $p < 0.0001$ , respectively, Fisher's exact test). Thus, the DNA methylation status of

the *UGT1A1* promoter region is different in the liver and kidney.

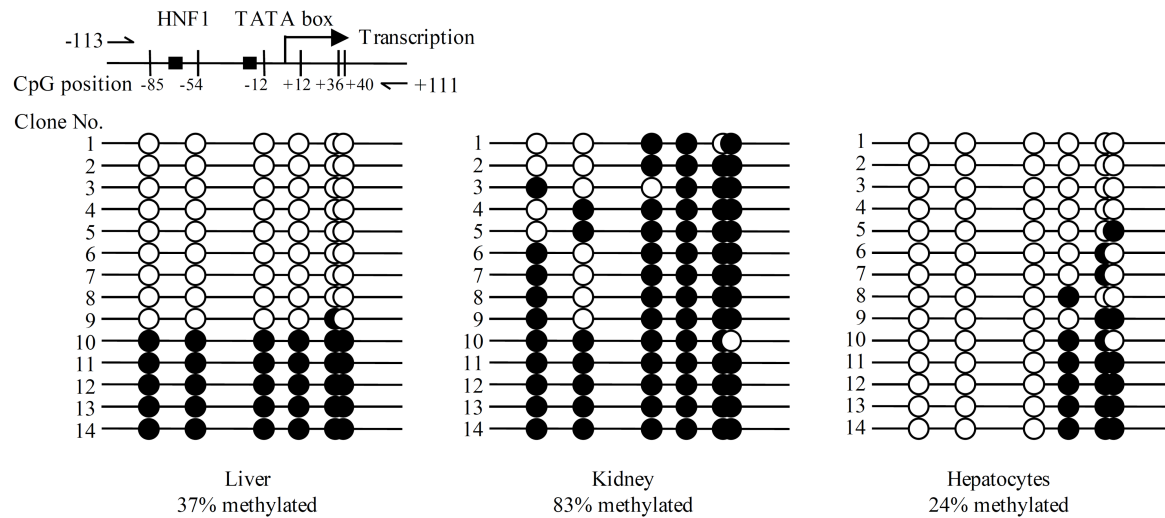


**Fig. 9.** DNA methylation status of the *UGT1A1* promoter region in human liver, kidney or hepatocytes. Top, a schematic diagram of the *UGT1A1* 5'-flanking region. The vertical lines and numbers represent the position of the cytosine residues of the CpGs relative to the TSS as +1. The HNF1 binding site and TATA box are represented by rectangles. Arrows indicate the positions of the primers used for ChIP analysis. Bottom, DNA methylation status of CpG sites. Bisulfite sequencing analysis was performed using genomic DNAs extracted from human liver (donor 3), kidney (donor 1) or hepatocytes (HH268). Fourteen clones from each sample type were sequenced. The open and closed circles represent unmethylated and methylated cytosines, respectively.

### Histone H3 acetylation status and recruitment of HNF1 $\alpha$ to the *UGT1A1* promoter region

DNA methylation induces chromatin condensation by recruiting chromatin-remodeling factors such as methyl-CpG-binding protein and histone deacetylase, thus limiting the access of transcription factors (Bird and Wolffe, 1999). ChIP assays were performed to determine the extent of histone H3 acetylation at the *UGT1A1* promoter in the liver and kidney. In addition, the extent of the recruitment of HNF1 $\alpha$  to the *UGT1A1* promoter in the liver and kidney was also determined because it has been demonstrated that HNF1 $\alpha$  regulates *UGT1A1* expression (Bernard et al., 1999). As shown in Fig. 10A, acetylated histone H3 was enriched at the *UGT1A1* promoter in the liver, but not in the kidney. In addition, it was demonstrated that HNF1 $\alpha$  was highly recruited to the *UGT1A1* promoter in the liver, but not in the kidney (Fig. 10B). Western blot analysis demonstrated that HNF1 $\alpha$  is expressed in kidney and liver equally (Fig. 10C). These results suggest that the DNA hypermethylation in the kidney could be linked to abolished histone H3 acetylation and HNF1 $\alpha$  binding.

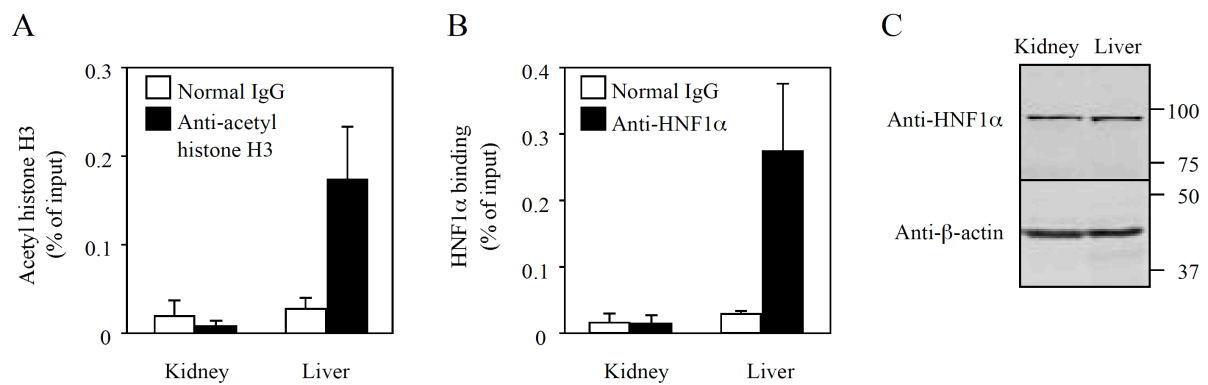


**Fig. 10.** Histone H3 acetylation and recruitment of HNF1 $\alpha$  in the *UGT1A1* promoter region in human kidney and liver. **(A and B)** ChIP assay of acetyl histone H3 and HNF1 $\alpha$  in kidney and liver. Human kidney (donor 1) and liver (donor 3) chromatin was precipitated with anti-acetyl histone H3 antibody **(A)** or anti-HNF1 $\alpha$  antibody **(B)**. The precipitated DNA was quantified by real-time PCR with a primer pair that amplified the region from -118 to +111 of the *UGT1A1* gene. The results are expressed as the percentage of input. Normal rabbit or goat IgGs (open columns) were included as negative controls. **(C)** Western blot analysis of HNF1 $\alpha$  in kidney and liver. Homogenates (50  $\mu$ g) from kidney and liver samples were subjected to 10% SDS-PAGE and probed with anti-HNF1 $\alpha$  or anti- $\beta$ -actin antibodies. Each column represents the mean  $\pm$  SD of triplicate determinations.

### Effects of the inhibition of DNA methylation and histone deacetylation and the transfection of exogenous HNF1 $\alpha$ on UGT1A1 expression

To investigate the significance of the DNA methylation at the promoter region in the repression of UGT1A1 expression, a series of experiments using cell lines was performed. Two cell lines, the human kidney-derived HK-2 line and liver-derived HuH-7 cells, were selected. It was found that the *UGT1A1* promoter region was hypermethylated (98%) in HK-2 cells but was moderately methylated (47%) in HuH-7 cells ( $p < 0.0001$ , Fig. 11A). UGT1A1 mRNA was marginally expressed in HK-2 cells but was substantially expressed in HuH-7 cells (~4800 fold difference) (Fig. 11B), suggesting that DNA methylation negatively regulates UGT1A1 expression in HK-2 cells. To investigate whether the inhibition of DNA methylation could induce UGT1A1 expression, the cells were treated with 5-Aza-dC, an inhibitor of DNA methylation. Although this treatment increased UGT1A1 mRNA in both cell lines, the induction was higher in HK-2 cells (~400 fold at maximum) than in HuH-7 cells (~6 fold at maximum) (Fig. 11B). It was confirmed that 5-Aza-dC treatment efficiently decreased the methylation status in HK-2 to 33% ( $p < 0.001$ ) and in HuH-7 cells to 7% ( $p < 0.001$ ) (Fig. 11C).

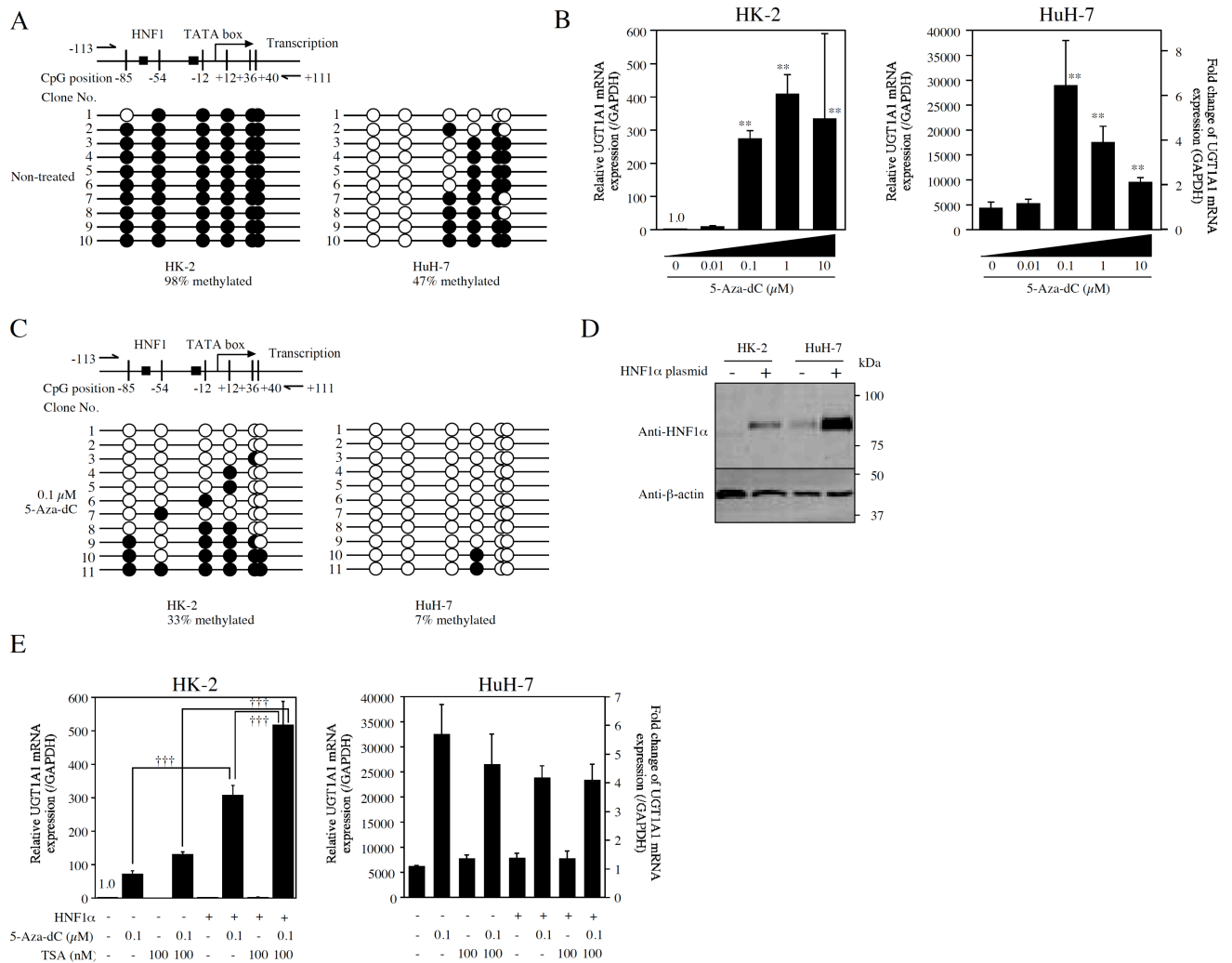


**Fig. 11.** Effects of 5-Aza-dC and/or TSA treatment and transfection of HNF1a on the UGT1A1 expression in HK-2 and HuH-7 cells. **(A)** DNA methylation status of the *UGT1A1* promoter region in HK-2 and HuH-7 cells. Ten clones each were sequenced. The open and closed circles represent unmethylated and methylated cytosines, respectively. **(B)** Effects of 5-Aza-dC on the UGT1A1 expression in HK-2 and HuH-7 cells. UGT1A1 mRNA level was determined by real-time RT-PCR and normalized to the GAPDH mRNA levels. **(C)** Effects of 5-Aza-dC on the DNA methylation status of the *UGT1A1* promoter region in HK-2 and HuH-7 cells. Bisulfite sequencing analysis was performed using genomic DNA extracted from 5-Aza-dC-treated cells. **(D)** Western blot analysis of HNF1 $\alpha$  in HK-2 and HuH-7 cells. Nuclear extracts from HK-2 and HuH-7 cells transfected with HNF1 $\alpha$  expression plasmid (+) or empty plasmid (-) were analyzed. **(E)** Effects of 5-Aza-dC and/or TSA treatment and transfection of HNF1 $\alpha$  on the UGT1A1 mRNA expression in HK-2 and HuH-7 cells. The cells were transiently transfected with HNF1 $\alpha$  expression plasmid (+) or empty plasmid (-), followed by treatment with 5-Aza-dC and/or TSA. The expression level of UGT1A1 mRNA was determined by real-time RT-PCR. Data were expressed as relative to UGT1A1 expression compared with non-treated HK-2 cells. Each column represents the mean  $\pm$  SD of triplicate determinations. \*\* $p < 0.01$ , compared with non-treated cells. ††† $p < 0.001$ .

The UGT1A1 mRNA level in HK-2 cells treated with 0.1  $\mu$ M 5-Aza-dC was still low in comparison to that in HuH-7 cells. It was suspected that HNF1 $\alpha$  might be lacking in HK-2 cells, thus causing the lower UGT1A1 levels. Western blot analysis demonstrated that HNF1 $\alpha$  is expressed at very low levels in HK-2 cells (Fig. 11D). To investigate the

significance of the DNA methylation status in the suppression of UGT1A1 expression, HNF1 $\alpha$  was exogenously expressed in HK-2 cells. The HNF1 $\alpha$  protein level was dramatically increased by the transfection of the HNF1 $\alpha$  expression plasmid into HK-2 cells (Fig. 11D), but UGT1A1 mRNA expression was not increased (Fig. 11E). These results suggested that DNA methylation inhibits the binding of HNF1 $\alpha$  to the promoter of *UGT1A1*. However, under 5-Aza-dC treatment, the overexpression of HNF1 $\alpha$  resulted in a significant increase of UGT1A1 mRNA expression (4.3 fold) in HK-2 cells. This phenomenon was not observed in HuH-7 cells, implying that endogenous HNF1 $\alpha$  expression levels might be sufficient for UGT1A1 in HuH-7 cells (Fig. 11D).

Finally, it was investigated whether histone deacetylation is also involved in the repression of UGT1A1 expression. When the HK-2 and HuH-7 cells were treated with TSA, an inhibitor of histone deacetylation, UGT1A1 mRNA expression was unchanged (Fig. 11E). However, TSA treatment facilitated (by 1.7 fold) the increase of UGT1A1 mRNA by 5-Aza-dC treatment in HK-2 cells in the presence of exogenously expressed HNF1 $\alpha$ . This result was not observed in HuH-7 cells. Collectively, these results suggest that DNA methylation status, and to a lesser extent histone deacetylation status, are critical determinants of UGT1A1 expression.

## **DISCUSSION**

Human UGT1A1 is predominantly expressed in the liver and the intestine, but not in the kidney. Previous studies demonstrated that HNF1 $\alpha$  and HNF1 $\beta$  are involved in the constitutive (Bernard et al., 1999) and inducible expression of UGT1A1 (Sugatani et al., 2008) by binding to a site approximately 30 bp upstream of the TATA box. The expression of HNF1 $\alpha$  and HNF1 $\beta$  is not confined to the liver, as these genes are expressed in various tissues including the kidney, intestine, stomach, and pancreas (Harries et al., 2006). Therefore, the reason for the repressed expression of UGT1A1 in the kidney remained to be clarified. To uncover the underlying mechanism, this study was conducted focusing on epigenetic regulation. HNF1 $\alpha$  and HNF1 $\beta$  form homodimers or heterodimers, and equally *trans*-activate

the *UGT1A1* gene (Bernard et al., 1999). Therefore, HNF1 $\alpha$  was focused as the representative *UGT1A1* activator.

It was demonstrated that the CpG island at the promoter region of the *UGT1A1* gene in the kidney was hypermethylated, whereas it was hypomethylated in the liver (Fig. 9). Upon DNA methylation, gene silencing occurs by two mechanisms: 1) the methyl group physically interrupts the binding of transcription factors to their recognition sequences, and 2) methyl-CpG-binding proteins bind to the methylated DNA and recruit corepressor molecules including histone deacetylase to induce chromatin structure condensation (Shiota, 2004). Previously, it was shown by gel shift assay that the methylated CpG sites at the *UGT1A1* promoter did not prevent the binding of HNF1 $\alpha$  (Bélanger et al., 2010). In contrast, the present study demonstrated that DNA hypermethylation of the *UGT1A1* promoter in the kidney was accompanied by increased acetylation of histone H3 and defective recruitment of HNF1 $\alpha$  (Fig. 10). Therefore, gene silencing of UGT1A1 in the kidney would be due to the latter mechanism with the abolished binding of HNF1 $\alpha$ .

The cell lines based study clearly demonstrated the significance of DNA methylation in the regulation of UGT1A1 as follows: 1) substantial expression of UGT1A1 mRNA is observed in HuH-7 cells with DNA hypomethylation status, 2) 5-Aza-dC treatment resulted in an increase of UGT1A1 expression that reflected the change in methylation status, and 3) the exogenously expressed HNF1 $\alpha$  could increase UGT1A1 expression only in the presence of 5-Aza-dC in HK-2 cells. These findings clearly illustrated that unmethylated DNA is a prerequisite for the transcriptional activation of UGT1A1.

The study using TSA demonstrated that histone acetylation is a supplemental factor for transactivation, supporting the general perception (Cameron et al., 1999). In contrast to the present study, a previous study reported a significant increase of UGT1A1 mRNA expression following treatment with 3 mM TSA in HepG2 cells (Mackenzie et al., 2010). When the HK-2 and HuH-7 cells were treated with 1 mM TSA, a prominent decrease of cell viability was observed (data not shown). Thus, it is possible that there are inter-cell line differences in the response toward TSA. Collectively, DNA methylation at the promoter region of *UGT1A1*

may evoke the condensed chromatin structure through histone deacetylation, thereby inhibiting the binding of transcription factors such as HNF1 $\alpha$ . This theory would explain the defective expression of UGT1A1 in kidney, where HNF1 $\alpha$  is substantially expressed.

Although the simultaneous overexpression of HNF1 $\alpha$  and inhibition of DNA methylation tremendously induced UGT1A1 mRNA in HK-2 cells, the UGT1A1 level was still lower than the level in HuH-7 cells (Fig. 11). It was surmised that some factors regulating UGT1A1 expression might be insufficient in HK-2 cells. Previous studies have reported that pregnane X receptor (Sugatani et al., 2008), glucocorticoid receptor (Usui et al., 2006), constitutive androstane receptor (Sugatani et al., 2008), peroxisome proliferator-activated receptor  $\alpha$  (Senekeo-Effenberger et al., 2007), NF-E2-related factor-2 (Yueh and Tukey, 2007), and aryl hydrocarbon receptor (Yueh et al., 2003) are involved in UGT1A1 regulation. It is possible that such factors may be insufficient in HK-2 cells, although experimental proof is required. As another possibility, differences in histone modifications other than acetylation, namely H3K4 methylation (activating mark), H3K9 methylation (silencing mark), and H3K27 methylation (silencing mark), are feasible. Thus, such factors might also be involved in the regulation of the basal expression of UGT1A1 in cell lines and tissues.

Each member of UGT1A family has a unique promoter. The tissue-specific expression of UGT1As could be attributed to the differences in their promoter activation (Gong et al., 2001). It is reasonable to assume that UGT isoforms other than UGT1A1 showing tissue-specific expression might also be epigenetically regulated.

In conclusion, the present study clearly demonstrated that the DNA methylation status of the human *UGT1A1* promoter is different in the liver and kidney. DNA methylation, hypoacetylation of histone H3, and diminished binding of HNF1 $\alpha$  could explain the defective expression of UGT1A1 in the kidney. A remaining future challenge is the elucidation of the effects of factors affecting epigenetic status such as aging, sex, disease, and habits on UGT1A1 expression.

## CHAPTER 4

### Tissue-specific expression of human UGT1A10 by epigenetic regulation

#### ABSTRACT

Human UDP-glucuronosyltransferase (UGT) 1A10 is not expressed in liver, but is exclusively expressed in the intestine, contributing to presystemic first-pass metabolism. Earlier studies revealed that hepatocyte nuclear factor (HNF) 1 $\alpha$  and Sp1 as well as an intestine-specific transcription factor, caudal type homeobox (Cdx) 2 are involved in the constitutive expression of UGT1A10. However, the reason why UGT1A10 is not expressed in the liver in which HNF1 $\alpha$  and Sp1 are abundantly expressed remains unknown. The purpose of this study was to uncover the mechanism of the tissue-specific expression of UGT1A10, focusing on its epigenetic regulation. Bisulfite sequence analysis revealed that the CpG-rich region (-264 to +117) around the *UGT1A10* promoter was hypermethylated (89%) in the epithelium of small intestine, whereas it was hypomethylated (6%) in the hepatocytes. Luciferase assay revealed that methylation of the *UGT1A10* promoter by *SssI* methylase abrogated transactivity even with the overexpressed Cdx2 and HNF1 $\alpha$ . The *UGT1A10* promoter was highly methylated (86%) in liver-derived HuH-7 cells in which UGT1A10 is not expressed, whereas that was hardly methylated (19%) in colon-derived LS180 cells in which UGT1A10 is expressed. Treatment with 5-Aza-dC, an inhibitor of DNA methylation, resulted in an increase of UGT1A10 mRNA expression only in HuH-7 cells. Moreover, overexpression of HNF1 $\alpha$  and Cdx2 further increased UGT1A10 mRNA only in the presence of 5-Aza-dC. A ChIP assay demonstrated that H3K27 around the promoter was trimethylated in the liver but not in the small intestine. In summary, this study found that DNA hypermethylation and H3K27 trimethylation would interfere with binding of HNF1 $\alpha$  and Cdx2, resulting in the defective expression of UGT1A10 in the human liver. Epigenetic regulation is a crucial determinant of tissue-specific expression of UGT1A10.

## **INTRODUCTION**

Human UGT enzymes are expressed in a tissue-specific manner. Most UGTs including UGT1A1, UGT1A3, UGT1A4, UGT1A6, UGT1A9, UGT2B4, and UGT2B7 are predominantly expressed in the liver (Izukawa et al., 2009; Court et al., 2012) and to a lesser extent expressed in extrahepatic tissues. Several UGTs are preferentially expressed in extrahepatic tissues, including kidney, small intestine, colon, stomach, lungs, ovaries, testis, mammary glands and prostate. In particular, UGT1A7, UGT1A8, and UGT1A10 are exclusively expressed in the gastrointestinal tract, but not in the liver. This expression limits the bioavailability of orally administered drugs such as raloxifene, naloxon, and mycophenolic acid as well as xenobiotics such as resveratrol and quercetin (Ritter, 2007; Basu et al., 2004). To elucidate the underlying mechanisms of tissue-specific expression of UGTs, some studies were conducted focusing on transcriptional regulation (Gardner-Stephen and Mackenzie, 2008; Mackenzie et al., 2010). It has been demonstrated that the intestine-specific transcription factor, Cdx2, Sp1, and HNF1 $\alpha$  regulate UGT1A8 and UGT1A10 expression in the intestine (Gregory et al., 2003, 2004a and 2004b). However, a question why UGT1A10 is not expressed in the liver even though HNF1 $\alpha$  is abundantly expressed remains unsolved. The purpose of this study is to clarify the mechanisms underlying the defective expression of UGT1A10, focusing on epigenetic regulation.

## **MATERIAL AND METHODS**

### **Chemicals and reagents**

5-Aza-dC, TSA, BIX-01294 trihydrochloride, and 3-deazaneplanocin A hydrochloride (Dznep) were purchased from Sigma-Aldrich. Goat anti-human HNF1 $\alpha$  polyclonal antibody (C-19), goat anti-human Cdx2 polyclonal antibody (C-20), and control rabbit and goat IgGs were purchased from Santa Cruz Biotechnology. Rabbit anti-trimethyl-Histone H3 (Lys27) polyclonal antibody (07-449) was purchased from Millipore. Primers were commercially synthesized at Hokkaido System Science. All other chemicals and solvents were of the highest grade commercially available.

## **Human tissues**

Human liver (a 39-year-old Japanese female) and small intestine (a 49-year-old Caucasian female) were obtained from autopsy materials that were discarded after pathological investigation. The use of the human livers and small intestines was approved by the Ethics Committees of Kanazawa University (Kanazawa, Japan) and Iwate Medical University (Morioka, Japan).

## **Cell culture**

Colorectal adenocarcinoma cell lines LS180, Caco-2, HT-29, and SW480, and a hepatocellular carcinoma cell line HepG2 were obtained from the American Type Culture Collection (Manassas, VA). A hepatocellular carcinoma cell line HuH-7 was obtained from the RIKEN BioResource Center. HT-29 and SW480 cells were cultured in RPMI1640 (Nissui Pharmaceutical, Tokyo, Japan) supplemented with 10% fetal bovine serum (FBS) (Invitrogen, Carlsbad, CA). The other cells were cultured as previously described (Nakamura et al., 2008).

## **RNA isolation and real-time RT-PCR**

Total RNA was isolated from cell lines using RNAiso (Takara Bio) according to the manufacturer's protocol. The cDNA was synthesized from the total RNA using ReverTraAce (Toyobo). The UGT1A10 mRNA levels were determined by real-time RT-PCR and normalized to GAPDH mRNA levels as described previously (Izukawa et al., 2009).

## **Genomic DNA extraction and bisulfite reaction**

Genomic DNA samples were prepared from human hepatocytes (HH268, a 54-year-old Caucasian female, Tissue Transformation Technologies), whole small intestine or epithelium of small intestine, and cell lines with a Genra Puregene Tissue kit (Qiagen). Five hundred nanograms of genomic DNA digested with *EcoR* I was treated with bisulfite using the EZ DNA Methylation kit (Zymo Research). The DNA fragments spanning the TSS of the *UGT1A10* or *UGT1A8* genes and the 5'-flanking region of *UGT1A9* were amplified by PCR

using the primer pairs shown in Table 5. The PCR products were cloned into the pT7Blue T-Vector (Novagen, Madison, WI). Since the primer pair for bisulfite analysis of UGT1A8 and UGT1A10 amplifies the corresponding regions of not only UGT1A8 and UGT1A10 but also UGT1A9, clones containing UGT1A9 sequence were precluded by digestion with an appropriate restriction enzyme and clones containing UGT1A8 or UGT1A10 sequences were subjected to sequence analysis. The DNA methylation status of the sequence was analyzed using the web-based tool QUMA (Kumaki et al., 2008).

**Table 5.** Sequences of oligonucleotides used in the present study.

Oligonucleotides	5' to 3' sequence	Position
Bisulfite analysis of UGT1A8 and UGT1A10		
Forward	AGAGAGTATTTGGTTGGTTAAAG	-365 to -343 <sup>a</sup>
Reverse	ACACTACCAACAACCTCCCTACC	+118 to +140 <sup>a</sup>
Bisulfite analysis of UGT1A9		
Forward	TTTGAAGGAGGGTATTGGAGTGATG	-754 to -730
Reverse	CCAAACCCTAAAAACCTCTAAAATAC	-540 to -514
Cloning of promoter region of UGT1A10		
Forward	CTTTGGATCCAGAGAGTATTTGGTTGGC	-365 to -347
Reverse	CCATAGATCTGCACTACCAGCAGCTTCCC	+122 to +140
Cloning of promoter region of UGT1A9		
Forward	GGCAGCTGCAGTTGATCTTTTCCCTTTAAG	-955 to -937
Reverse	CAGAGATCTGCAGCTGAGAG	+17 to +29
ChIP assay of UGT1A10		
Forward	AATGATACTCGTGTGTATC	-135 to -116
Reverse	AGACACACACATAAAGGAAC	+76 to +95
Cloning of Cdx2		
Forward	CCGGACCCTCGCCACCATGTA	-16 to +5
Reverse	GTGGGTCACTGGGTGACGGT	+927 to +947

Nucleotides are numbered with the TSS designated as +1 in the genomic DNA sequence of UGTs and base A in the initiation codon ATG designated as +1 in the Cdx2 cDNA sequence. The restriction sites used for cloning are underlined. The restriction sites used for cloning are underlined.

<sup>a</sup> The numbers refer to the nucleotide position of *UGT1A10*.

### Construction of expression plasmids and luciferase reporter plasmids

A luciferase reporter plasmid, pCpGL-basic, which completely lacks CpG dinucleotides, was kindly provided by Dr. Rehli (Klug and Rehli, 2006). The 5'-flanking regions of

*UGT1A9* (-955 to +29) or promoter region of *UGT1A10* (-365 to +140) amplified by PCR using human liver genome as a template was cloned into the pCpGL-basic plasmid and the products were termed UGT1A9/pCpGL and UGT1A10/pCpGL, respectively. HNF4 $\alpha$  and HNF1 $\alpha$  expression plasmids were constructed in the previous study (Takagi et al., 2010) and in chapter 3, respectively. For the construction of Cdx2 expression plasmid, human Cdx2 cDNA was amplified by PCR using the primer pair shown in Table 5 with human small intestine cDNA as a template. The PCR product was subcloned into the pTARGET vector (Promega, Madison, MI). The nucleotide sequence was confirmed by DNA sequencing analysis.

### **Luciferase reporter assays**

The pCpGL-basic, UGT1A9/pCpGL, and UGT1A10/pCpGL plasmids were treated with a CpG methylase *SssI* (New England Biolabs, Beverly, MA). For the luciferase assays, HuH-7 cells were seeded onto a 24-well plates at  $1 \times 10^5$  cells/well. After 24 h, 200 ng of pCpGL-basic plasmid and 300 ng each of human Cdx2, HNF1 $\alpha$ , and HNF4 $\alpha$  expression plasmids or pTARGET empty plasmid were transfected into the cells using Lipofectamine 2000 (Invitrogen). The cells were harvested 48 h after the transfection and lysed to measure the luciferase activity using a Dual Luciferase Reporter Assay System (Promega). The protein concentration was determined using Bradford protein assay reagent with  $\gamma$ -globulin as a standard. The relative luciferase activities were normalized to the protein content.

### **Chemical treatment and transfection of expression plasmid into the cells**

HuH-7 or LS180 cells were seeded onto a 12-well plate at  $0.5 \times 10^5$  cells/well and incubated for 24 h. For dose response experiments, the cells were treated with 0.01 to 10  $\mu$ M 5-Aza-dC for 120 h, 0.1 to 5  $\mu$ M BIX-01294 or Dznep for 120 h, or treated with 50 to 300 nM TSA for 24 h, and then subjected to RNA isolation. For the overexpression of HNF1 $\alpha$  and Cdx2, the cells were treated with 0.1  $\mu$ M 5-Aza-dC for 120 h. Sixty hours before harvesting, the cells were transiently transfected with 0.5  $\mu$ g of an HNF1 $\alpha$  and/or Cdx2 expression

plasmids using the X-tremeGENE HP DNA transfection reagent. The UGT1A10 mRNA levels were determined as described above.

### **Western blot analysis of HNF1 $\alpha$ and Cdx2**

Total cell homogenates (40  $\mu$ g) from HuH-7 and LS180 cells transfected with HNF1 $\alpha$  and Cdx2 expression plasmids were separated by 10% SDS-PAGE and transferred to an Immobilon-P transfer membrane. The membranes were probed with goat anti-human HNF1 $\alpha$  or rabbit anti-human Cdx2 antibodies followed by fluorescent dye-conjugated second antibodies. The membranes were then scanned using the Odyssey Infrared Imaging system.

### **ChIP assay**

The ChIP assay of trimethylation at H3K27 (H3K27me3) around *UGT1A10* TSS in human liver or epithelium of small intestine samples was performed as previously described (Oda et al., *in press*). Rabbit anti-H3K27me3 antibodies (07-449) and normal rabbit IgG were used for immunoprecipitation of the protein–DNA complexes. The -135 to +95 region of the *UGT1A10* gene was amplified by real-time PCR with the primers shown in Table 5. The protocol for the PCR was as follows: 95°C for 30 s followed by 45 cycles of 94°C for 4 s and 64°C for 20 s. DNA extraction and real-time PCR were also performed for the input samples, and the data were used as a control to evaluate the enrichment of DNA in the immunoprecipitates.

### **Statistical analyses**

For DNA methylation status, the statistical significance was evaluated by the Mann-Whitney *U*-test or Fisher's exact test using the web-based tool QUMA. For mRNA expression and luciferase assay, statistical significance was determined using an unpaired, two-tailed Student's *t* test or one-way analysis of variance followed by Dunnett's test. Correlation analyses were performed by the Spearman's rank method. When the *p* value was less than 0.05, the differences were considered to be statistically significant.

## RESULTS

### DNA methylation status of the 5'-flanking regions of *UGT1A8*, *UGT1A9*, and *UGT1A10* in human hepatocytes and small intestine

The location of CpG dinucleotides were searched from 300 bp upstream to 200 bp downstream of the TSS for human *UGT1A8*, *UGT1A9*, and *UGT1A10* genes (Fig. 12A). Five and 12 CpG dinucleotides were found around TSS (-365 to +140 bp) for *UGT1A8* and *UGT1A10*, respectively, whereas only two CpG dinucleotides were observed around TSS for *UGT1A9*. In the case of *UGT1A9*, there were multiple CpG dinucleotides spanning 800 to 600 bp upstream of the TSS. The DNA methylation status of the promoter regions of *UGT1A10* spanning -365 to +140 in the small intestine and liver was determined by bisulfite sequence analysis (Fig. 12B). Because my previous study demonstrated that the use of liver tissue sample displayed a mixed pattern of DNA methylation in parenchymal and non-parenchymal cells (Oda et al., *in press*), this study used human hepatocytes for the analysis. As shown in Fig. 12B, 89% of CpG sites (128 out of 144 CpG sites) in the promoter region of the *UGT1A10* gene were methylated in hepatocytes, whereas, 51% of CpG sites (86 out of 168 CpGs) were methylated in the whole small intestine. Notably, in the whole small intestine, the methylated CpG sites were biased in specific clones. It was surmised that these clones showing hypermethylation might be from submucosa of small intestine, where UGT enzymes are not expressed (Strassburg et al., 2000). Hence, epithelium cells prepared from small intestine was used to determine the DNA methylation status of the *UGT1A10* promoter. The methylation status was found to be only 11% (18 out of 168 CpG sites). Collectively, the DNA methylation status of the *UGT1A10* promoter region was found to be quite lower in the small intestine epithelium than hepatocytes ( $p < 0.0001$ , Mann-Whitney *U*-test).

Next, DNA methylation status of promoter of *UGT1A8*, which shows highly sequence similarity with *UGT1A10*, was investigated (Fig. 12B). In the promoter of *UGT1A8* from hepatocytes, 79% of CpG sites (51 out of 65 CpG sites) were methylated whereas in the small intestine epithelium, 16% of CpG sites (9 out of 55 CpGs) were methylated ( $p = 0.0004$ , Mann-Whitney *U*-test). The difference in DNA methylation pattern of *UGT1A8* between two

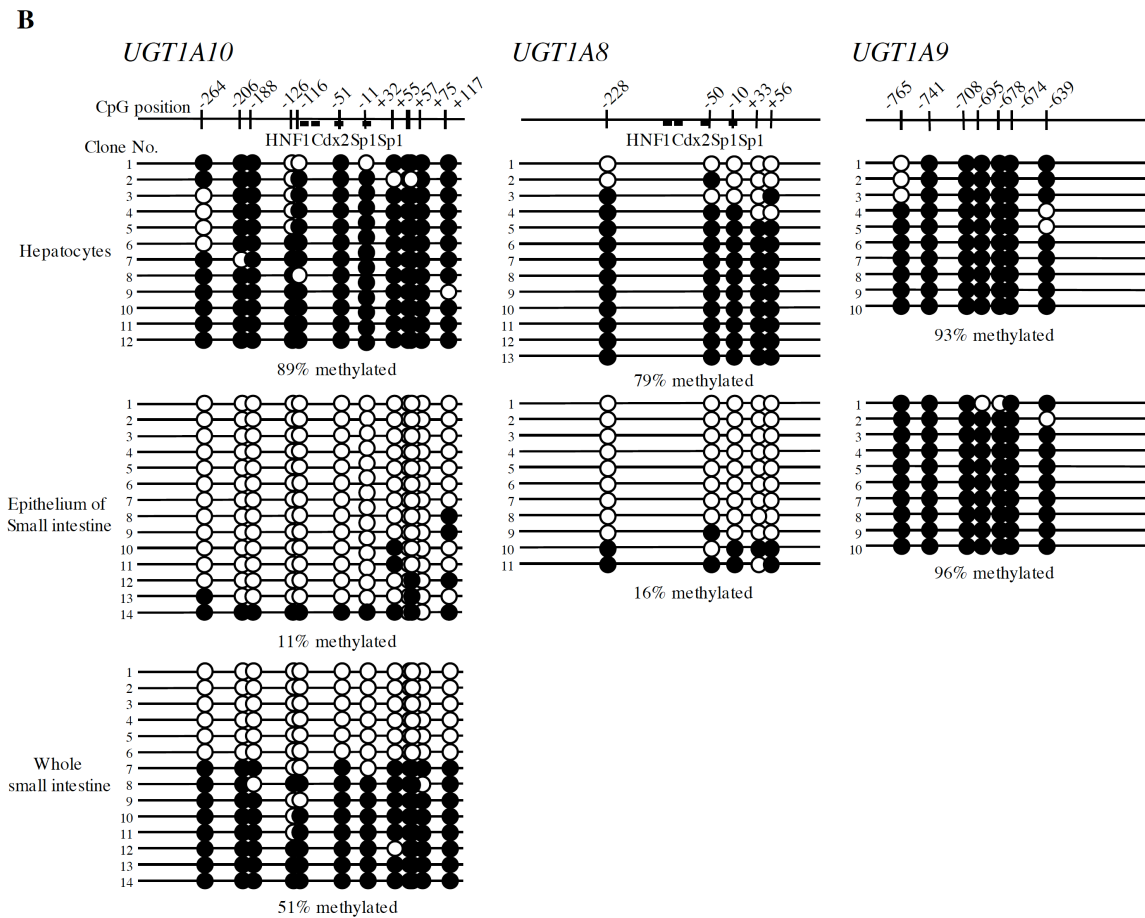
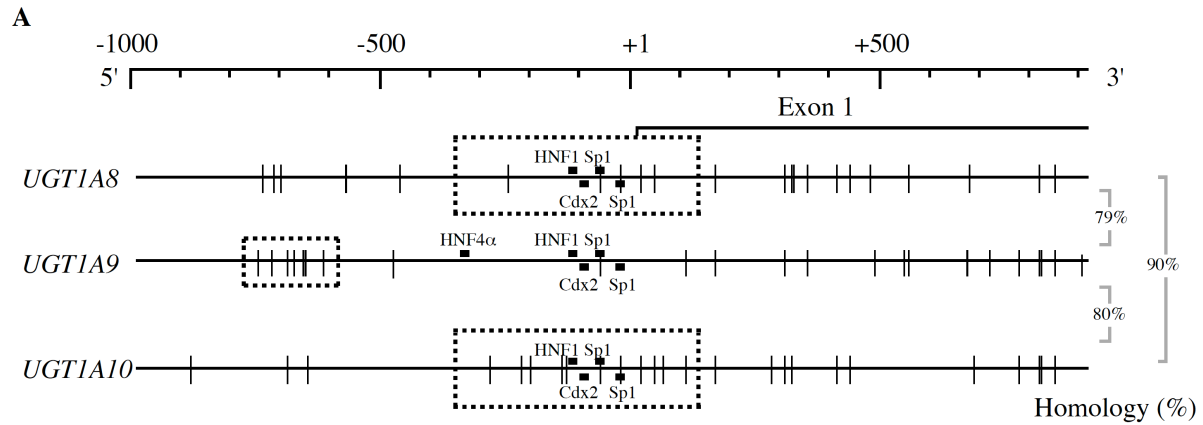


**Fig. 12.** DNA methylation status of *UGT1A8*, *UGT1A9*, and *UGT1A10* in human small intestine and hepatocytes. (A) A schematic diagram of the 5'-flanking region of *UGT1A8*, *UGT1A9*, and *UGT1A10*. The vertical lines and numbers represent the position of the cytosine residues of the CpGs relative to the TSS as +1. The transcription factor binding sites are represented by rectangles. Bisulfite sequence was performed in the region outlined with dashed rectangles. (B) DNA methylation status of CpG sites. Bisulfite sequencing analysis was performed using genomic DNAs extracted from human small intestine epithelium (donor 1) or hepatocytes (HH268). For *UGT1A10*, DNA methylation status in the genomic DNAs extracted from total small intestine was also investigated. At least ten clones from each sample type were sequenced. The open and closed circles represent unmethylated and methylated cytosines, respectively.

tissues was almost identical to that of UGT1A10. Because there are only two CpG sites in the promoter of *UGT1A9*, we investigated the further upstream CpG-rich region (-765 to -639 bp) for DNA methylation status. In the 5'-flanking region of *UGT1A9* from hepatocytes, 93% of CpG sites (65 out of 70 CpG sites) were methylated and in the small intestine epithelium, 96% of CpG sites (67 out of 70 CpGs) were methylated ( $p = 0.34$ , Mann-Whitney *U*-test). Thus, DNA methylation status of this region would not be associated with tissue-specific expression of UGT1A9.

### **Effects of DNA methylation on transactivity of *UGT1A10* and *UGT1A9***

To determine the effects of DNA methylation on the promoter activity, luciferase assays were performed using methylated and unmethylated luciferase constructs (Fig. 13). In the case of unmethylated UGT1A10/pCpGL construct, overexpression of either Cdx2 ( $p < 0.05$ ) or HNF1 $\alpha$  ( $p < 0.01$ ) highly increased the luciferase activity, and synergistic increase of the activity was observed by coexpression of these factors ( $p < 0.01$ ), supporting the previous study (Gregory et al., 2004a). In the case of the methylated UGT1A10/pCpGL construct, overexpression of Cdx2 and/or HNF1 $\alpha$  did not significantly increased luciferase activities. Luciferase activities of unmethylated UGT1A10/pCpGL constructs were significantly higher than methylated constructs, indicating that DNA methylation status have a great impact on the transcriptional activity of UGT1A10. Overexpression of HNF4 $\alpha$  did not increase the luciferase activity of UGT1A10. This would be because the sequence of the HNF4 $\alpha$  recognition element in the *UGT1A10* gene was different by one nucleotide from the consensus HNF4 $\alpha$  response element sequence (Barbier et al., 2005). In the case of UGT1A9/pCpGL construct, the overexpressed HNF4 $\alpha$  increased ( $p < 0.01$ ) the activity regardless of methylation status, although the overexpressed Cdx2 and HNF1 $\alpha$  did not significantly increase the luciferase activity. These results suggest that DNA methylation of 5'-flanking region was not associated with the transcriptional activity of UGT1A9.

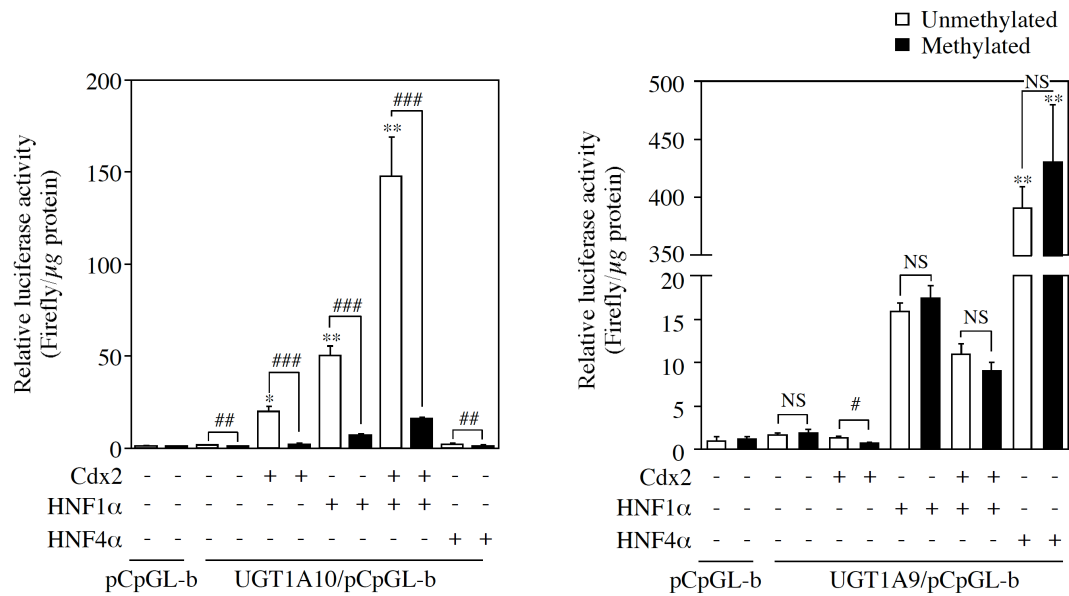


**Fig. 13.** Effects of DNA methylation on the transactivity of UGT1A10 and UGT1A9. pCpGL-basic plasmids containing either -365 to +140 of *UGT1A10* or -955 to +29 of *UGT1A9* as well as pCpGL-basic plasmid were treated with *Sss* I DNA methylase. Either the treated or untreated reporter construct and Cdx2, HNF1α or HNF4α expression plasmids were transiently transfected into HuH-7 cells. After 48 h, the cells were harvested and the luciferase activities were measured. Each column represents the mean  $\pm$  SD of relative activities (firefly/ $\mu$ g protein) of triplicate determinations. \*  $p < 0.05$  and \*\*  $p < 0.01$ , compared with no transfection. ##  $p < 0.01$  and ###  $p < 0.001$ , compared with unmethylated construct.

### DNA methylation status of the *UGT1A10* promoter regions in colon- or liver-derived carcinoma cell lines

DNA methylation status of the *UGT1A10* promoter region in six kinds of human cell lines: colon adenocarcinoma cell lines, LS180, Caco2, HT29, and SW480 and hepatocellular carcinoma cell lines, HepG2 and HuH-7 were investigated. The degree of DNA methylation in *UGT1A10* promoter was, in ascending order, HT-29 < LS180 < HepG2 < SW480 < HuH-7 < Caco-2 (Fig. 14). The expression level of *UGT1A10* mRNA in these cells was measured and relationship with DNA methylation status was analyzed. DNA methylation levels tended to be inversely correlated with the *UGT1A10* mRNA expression levels (Spearman's  $r = -0.54$ ,  $p = 0.29$ ). These results suggest that DNA methylation status would determine the basal expression level of *UGT1A10* in cell lines. In the subsequent experiments, two cell lines, the human colon adenocarcinoma LS-180 and hepatocellular carcinoma HuH-7 cells were selected as representatives of *UGT1A10*-positive and -negative cells, respectively.

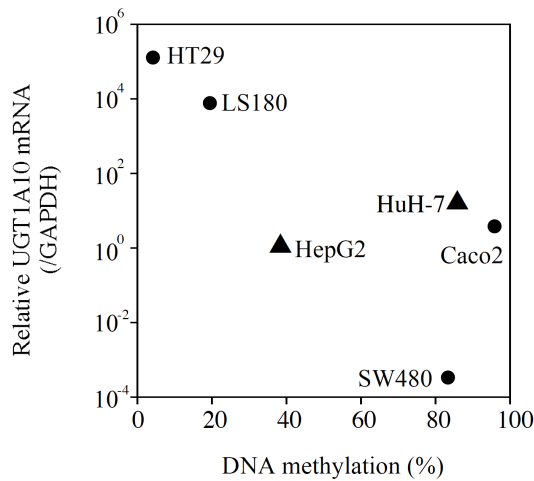


**Fig. 14.** Relationship between DNA methylation status of the promoter region of *UGT1A10* and mRNA expression levels of *UGT1A10* in colon- (circle) and liver-derived (triangle) carcinoma cells lines. DNA methylation status of *UGT1A10* was analyzed by bisulfite sequence analysis of at least five clones for each cell. Methylation status was expressed as percentage of methylated cytosines per total CpG dinucleotides among all the sequenced clones. The expression levels of *UGT1A10* mRNA were expressed as relative to levels in HepG2 cells.

### Effects of 5-Aza-dC and TSA on the *UGT1A10* mRNA expression

To investigate the significance of the DNA methylation at the promoter region in the *UGT1A10* expression, the experiments using epigenetic modulatory agents were performed. When these cells were treated with 5-Aza-dC, an inhibitor of DNA methylation for 5 days, *UGT1A10* mRNA expression was dramatically increased in HuH-7 cells (~16 fold at maximum), whereas was marginally increased in LS180 cells (~1.6 fold at maximum) (Fig. 15A). It was confirmed that 5-Aza-dC treatment decreased the methylation status in HuH-7 cells from 86% to 60% ( $p = 0.15$ ) (Fig. 15B). These results demonstrated that *UGT1A10* expression is silenced by DNA methylation. Unexpectedly, the methylation status in LS180 cells was slightly increased from 19% to 41% ( $p = 0.09$ ) by 5-Aza-dC treatment, although the reason is unknown (Fig. 15B). Next, the involvement of histone acetylation for the expression of *UGT1A10* was investigated. When these cells were treated with TSA, an inhibitor of histone deacetylase, for 1 day, the expression of *UGT1A10* mRNA was not increased in the both cell lines, suggesting histone acetylation has no impact on the *UGT1A10* regulation (Fig. 15A). The different expression level (~3-fold) of *UGT1A10* in LS180 cells between the controls for 5-Aza-dC and TSA treatment may be due to the difference in culture time.

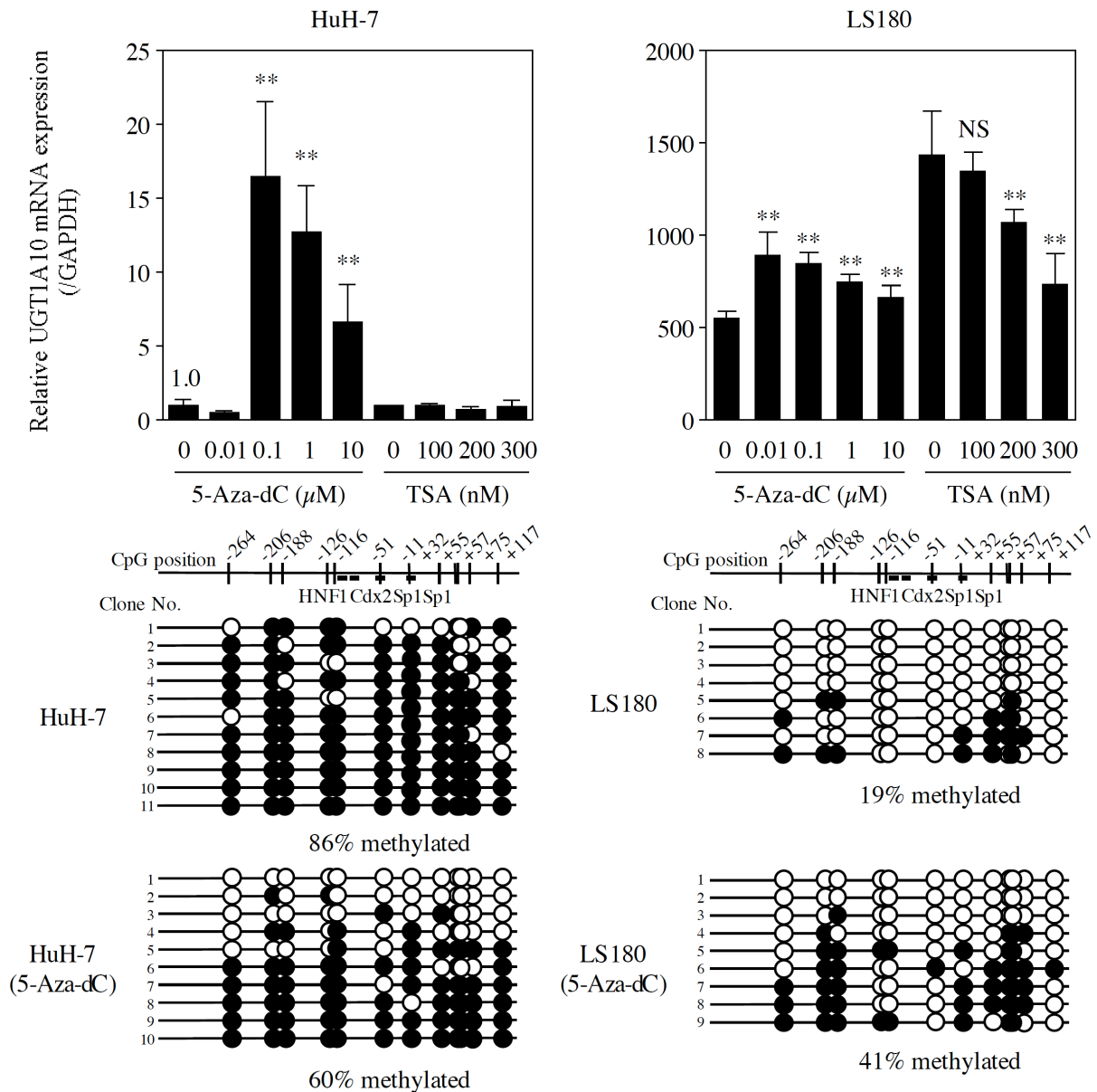


**Fig. 15.** Effects of 5-Aza-dC and/or TSA treatment on the UGT1A10 expression in HuH-7 and LS180 cells. (A) UGT1A10 mRNA levels in HuH-7 and LS180 cells treated with 5-Aza-dC or TSA, which were normalized to the GAPDH mRNA levels. Each column represents the mean  $\pm$  SD of triplicate determinations. \*\*  $p < 0.01$ , compared with non-treated cells. (B) DNA methylation status of the *UGT1A10* promoter region in HuH-7 and LS180 cells before and after the treatment with  $0.1 \mu\text{M}$  5-Aza-dC. Bisulfite sequencing analysis of at least eight clones for each cell was performed.

### Effects of 5-Aza-dC and overexpression of HNF1 $\alpha$ and Cdx2 on the UGT1A10 expression

It was investigated whether demethylation of DNA allows transcription factors to bind to the promoter of *UGT1A10* and thereby to activate the transcription (Fig. 16). In the intact

HuH-7 and LS180 cells, HNF1 $\alpha$  was marginally expressed, and Cdx2 was not expressed (Fig. 16). The transfection of the HNF1 $\alpha$  and Cdx2 expression plasmids into HuH-7 cells resulted in dramatic increase of HNF1 $\alpha$  and Cdx2 proteins (Fig. 16), but this did not increase the UGT1A10 expression (Fig. 16). However, under the 5-Aza-dC treatment, the overexpression of HNF1 $\alpha$  and Cdx2 resulted in a significant increase of UGT1A10 mRNA expression (11 fold) in HuH-7 cells. These results suggested that DNA methylation inhibits the binding of HNF1 $\alpha$  and Cdx2 to the promoter of *UGT1A10*. Overexpression of HNF1 $\alpha$  and Cdx2 under the 5-Aza-dC treatment did not result in upregulation of UGT1A10 in LS180 cells probably because extent of DNA methylation was originally low and the endogenous HNF1 $\alpha$  expression levels might be sufficient for the interaction with unknown components which might be essential for UGT1A10 expression in LS180 cells (Fig. 16).

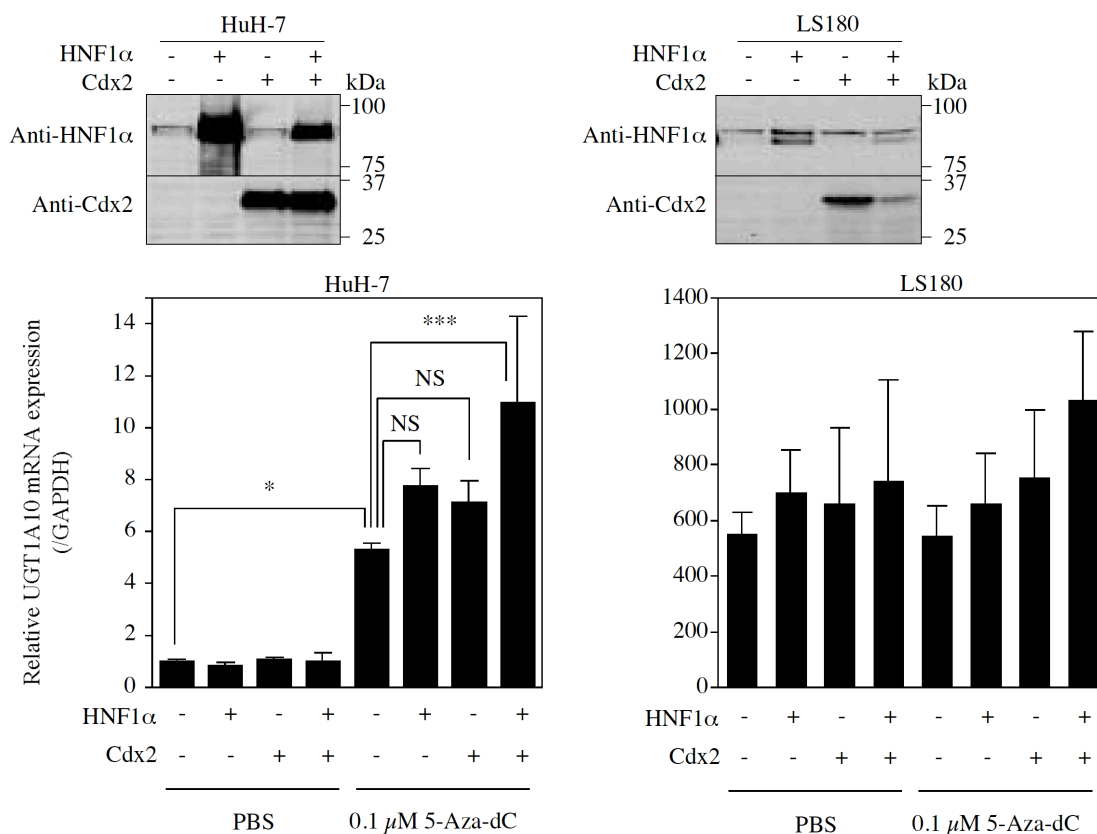


**Fig. 16.** Effects of 5-Aza-dC treatment and transfection of HNF1 $\alpha$  and Cdx2 on the UGT1A10 expression in HuH-7 and LS180 cells. The cells were treated with 5-Aza-dC followed by transient transfection of HNF1 $\alpha$  and/or Cdx2 expression plasmids (+) or empty plasmid (-). The expression level of UGT1A10 mRNA was determined by real-time RT-PCR. Data were expressed as relative to UGT1A10 expression compared with non-treated HuH-7 cells. The expression of HNF1 $\alpha$  and Cdx2 were analyzed by Western blot of total cell homogenates from the cells. Each column represents the mean  $\pm$  SD of triplicate determinations. \*  $p < 0.05$ , \*\*  $p < 0.01$ , and \*\*\*  $p < 0.001$ , compared with non-treated cells.

## Effects of histone methylation on the expression of UGT1A10

As another factor to repress UGT1A10 expression in the liver, histone methylation was surmised. Methylation at H3K9 and H3K27 is known to repress expression of a number of genes (Cedar and Bergman, 2009). When HepG2 cells were treated with BIX-01294, which was recently identified as an inhibitor of H3K9 methyltransferase G9a (Kubicek et al., 2007), UGT1A10 mRNA expression was unchanged (Fig. 17). In contrast, Dznep, which is an inhibitor of methylation of H3K27 (Tan et al., 2007), facilitated the UGT1A10 mRNA expression in a dose-dependent manner (Fig. 17), suggesting that H3K27 trimethylation was involved in the repressed expression of UGT1A10 in HepG2 cells.

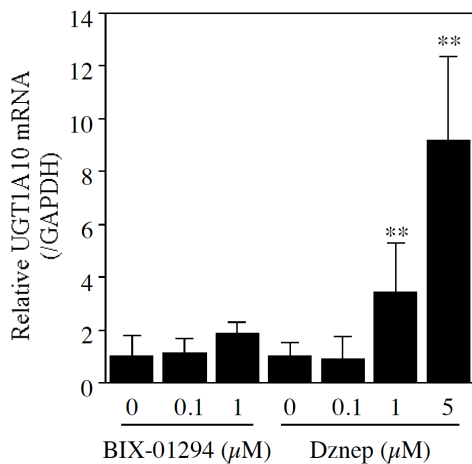


**Fig. 17.** Effects of BIX-01294 and Dznep treatment on the UGT1A10 expression in HepG2 cells. UGT1A10 mRNA level was determined by real-time RT-PCR and normalized to the GAPDH mRNA levels. Each column represents the mean  $\pm$  SD of triplicate determinations. \*\*  $p < 0.01$ , compared with non-treated cells.

## Trimethylation status of H3K27 in the promoter of *UGT1A10* in human small intestine and liver

ChIP assays were performed to investigate the trimethylation status of H3K27 in the promoter of *UGT1A10* in the liver and small intestine. As shown in Fig. 18, trimethylated H3K27 was enriched at the *UGT1A10* promoter in the liver, but not in the small intestine. It was considered that the H3K27me3 in the liver could be linked to silencing of UGT1A10, probably through hampering the binding of transcription factor such as HNF1 $\alpha$  to the promoter.

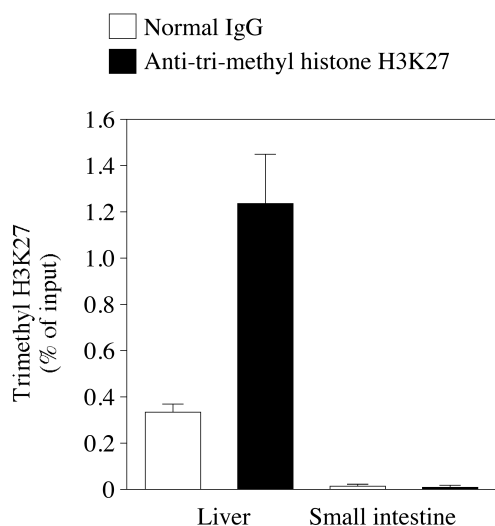


**Fig. 18.** Trimethylation of H3K27 in the promoter of *UGT1A10* in human liver and small intestine. ChIP assay of trimethyl H3K27 in the liver and small intestine. Human liver and small intestine chromatin was precipitated with anti-trimethyl H3K27 antibody. The precipitated DNA was quantified by real-time PCR with a primer pair that amplified the region from -135 to +95 of the *UGT1A10* gene. The results are expressed as the percentage of input. Normal rabbit IgG (open columns) was used as negative controls. Each column represents the mean  $\pm$  SD of triplicate determinations.

## DISCUSSION

Human *UGT1A10*, which is exclusively expressed in the small intestine and colon, but not in the liver, contributes to presystemic first-pass metabolism (Ritter, 2007; Mizuma, 2009). Previous studies demonstrated that HNF1 $\alpha$  and Sp1 as well as intestine-specific transcription factor Cdx2 are involved in the constitutive expression of *UGT1A10* (Gregory et al., 2003, 2004a and 2004b). However, HNF1 $\alpha$  and Sp1 cannot solely account for the intestine-specific expression of *UGT1A10*, because the expression of these transcription factors are not confined to intestines, but rather abundantly expressed in the liver, where *UGT1A10* is absent. In the present study, underlying mechanism of defective expression of *UGT1A10* in the liver was investigated focusing on the epigenetic mechanism.

It was demonstrated that the CpG-rich region at the promoter of the *UGT1A10* gene in the hepatocyte was hypermethylated, whereas it was hypomethylated in the small intestine epithelium (Fig. 12). Furthermore, reporter gene assays revealed that methylation of the *UGT1A10* promoter leads to an almost complete loss of transcriptional activity even under the overexpression of Cdx2 and HNF1 $\alpha$  (Fig. 13). These results clearly suggest that DNA methylation status is critical for *UGT1A10* expression. Cell lines-based studies clearly demonstrated the significance of DNA methylation in the regulation of *UGT1A10* as follows: 1) substantial expression of *UGT1A10* mRNA expression was observed in LS180 cells with DNA hypomethylation status, 2) 5-Aza-dC treatment resulted in the increase of *UGT1A10*

expression reflecting the change in DNA methylation status, and 3) exogenously expressed HNF1 $\alpha$  and Cdx2 could increase UGT1A10 expression only under the 5-Aza-dC treatment in HuH-7 cells (Figs. 15 and 16). These findings clearly illustrated that DNA methylation inhibits the expression of UGT1A10 and unmethylated DNA status is a prerequisite for the transcriptional activation of UGT1A10. With regard to UGT1A8, which is also expressed in the gastrointestinal tract but not liver as with UGT1A10, the promoter was hypomethylated in the small intestine epithelium and hypermethylated in the hepatocytes (Fig. 12). It was anticipated that the expression of UGT1A8 would be also regulated by DNA methylation, although the UGT1A8 expression was not examined in this study.

In general, gene silencing by DNA methylation is mediated by following two mechanisms: 1) the methyl group physically interrupts the binding of transcription factors to their recognition sequences, and 2) methyl-CpG-binding proteins bind to the methylated DNA followed by the recruitment of corepressor molecules including histone deacetylase to induce chromatin structure condensation (Shiota, 2004). In the case of UGT1A10, the former mechanism is unlikely to be involved, because there is no CpG dinucleotide in Cdx2 or HNF1 $\alpha$  recognition element at the *UGT1A10* promoter. Nevertheless the possibility that methylated CpGs outside the elements affect the binding of transcription factors could not be denied. The latter mechanism is also unlikely to be involved, because TSA treatment to inhibit histone deacetylation did not result in activation of UGT1A10 expression. Although this study has no exclusive explanation, the other mechanisms may be involved in the DNA methylation-dependent repression of UGT1A10.

Inhibition of DNA methylation and concomitant overexpression of HNF1 $\alpha$  and Cdx2 tremendously increased the UGT1A10 mRNA in HuH-7 cells. However, even under the condition, the UGT1A10 level was still lower than the level in intact LS180 cells (Fig. 16). The result prompted me to assume the involvement of other repressive chromatin modifications. To ensure this hypothesis, BIX-01294 and Dznep, which are inhibitor for methylation at H3K9 and H3K27, respectively, were added to the cells and found that Dznep increased the expression of UGT1A10 in HepG2 cells (Fig. 17). These results suggest that

trimethylation at H3K27 around *UGT1A10* promoter would be an additional underlying mechanism of the repressed expression of UGT1A10 in HepG2 cells. Trimethylation at H3K27 is mediated by Enhancer of zeste 2 (EZH2), the catalytic subunit of Polycomb repressive complex 2 (PRC2), while PRC1 is recruited to the H3K27me3 and is involved in gene silencing (Simon and Kingston, 2009). The presence of trimethylation at H3K27 in *UGT1A10* promoter in the liver and the absence in the small intestine further support the defective expression of UGT1A10 in liver (Fig. 18). Both DNA methylation and H3K27 trimethylation at the *UGT1A10* promoter were observed in liver. It is known that chromatin modifications and DNA methylation are strictly linked and can associate or interfere with each other (Klose and Bird, 2006). As for linkage between DNA methylation and H3K27 trimethylation, EZH2 directly recruits DNA methyltransferases to increase DNA methylation in cancer (Viré et al., 2006), which supports coexistence of these modifications of the *UGT1A10* promoter in liver. However, the generality of this mechanism is currently unclear as EZH2-mediated recruitment of DNA methyltransferases is not observed in all cancers or in normal cells (Reddington et al., 2013). Further study is needed to elucidate the association between DNA methylation and H3K27 trimethylation.

In contrast to UGT1A10 and UGT1A8, UGT1A9, of which promoter sequence (-1 kb from TSS) shares 80% and 79% similarity with those of *UGT1A10* and *UGT1A8* gene, respectively, is expressed in the liver but not in intestines. As supported by the present study (Fig. 13), it has been reported that UGT1A9 is not transactivated by Cdx2, but is transactivated by HNF1 $\alpha$  and HNF4 $\alpha$  (Gregory et al., 2004a; Barbier et al., 2005). The present study found that DNA methylation status at 5'-flanking region of *UGT1A9* was almost the same between the small intestine and liver (Fig. 12) and that the methylation status did not affect the transcriptional activity (Fig. 13). The results suggest that the DNA methylation in the 5'-flanking region of *UGT1A9* is not associated with the tissue-specific expression of UGT1A9. Although the reason of the defective expression of UGT1A9 in small intestine remains to be studied, the involvement of histone modification or repressive transcription factors may be possible.

The present study revealed that DNA methylation and trimethylation at H3K27 repress the expression of UGT1A10 in the liver. UGT1A10 mRNA was significantly lower in breast carcinoma than that in normal breast specimens (Starlard-Davenport et al., 2008). Since aberrant DNA methylation and H3K27 trimethylation patterns were observed in some cancers (Jones and Baylin, 2002; Sharma et al., 2010; Portela and Esteller, 2010), it is possible that the alteration of UGT1A10 expression in breast carcinoma can be explained by epigenetic mechanism. UGT1A10 is responsible for the detoxification of 4-(methylnitrosamino)-1-(3-pyridyl)-1-butanol (NNAL), a major procarcinogenic metabolite of the potent tobacco-specific nitrosamine 4-(methylnitrosamino)-1-(3-pyridyl)-1-butanone (NNK), as well as other potent carcinogens (Balliet et al., 2010), variation in UGT1A10 expression may be related with individual susceptibility to the carcinogenicity of these agents. Further studies are warranted to better understand the role of the epigenetic regulation of UGT1A10 in cancer susceptibility.

My previous study demonstrated that DNA hypermethylation and histone H3 hypoacetylation results in the defective expression of UGT1A1 in the kidney, revealing the impact of the epigenetic modification in the tissues-specific expression of UGT1A1 (Oda et al., *in press*). This study found that UGT1A10 expression is distinctly regulated by DNA methylation. Previous studies have revealed that the expression of UGT1A6, UGT2B15, and UGT2B28 (Dannenberg and Edenberg, 2006) and UGT2B7 and UGT2B11 (Valentini et al., 2007) in cancer cell lines were increased by treatment with 5-Aza-dC or valproate which is also a DNA methylation inhibitor. Although DNA methylation status of these five UGT isoforms has not been investigated, it is possible that tissue- or cell-specific expression of most UGTs may be epigenetically regulated.

In summary, this study found that DNA methylation and H3K27 trimethylation of the *UGT1A10* gene would limit the binding of transcription factors to repress the expression of UGT1A10 in liver. The findings provide novel mechanisms of the tissue-specific expression of UGT1A10.

## CHAPTER 5

### Conclusion

Glucuronidation is an important pathway for the clearance of therapeutic drugs, environmental toxins, and endogenous compounds from the body. The reaction is catalyzed by UGTs. There are 19 different human UGTs, which are expressed in various tissues including liver, kidney, small intestine, and brain. The purpose of this study was to generate isoform-specific antibodies and to investigate the interindividual variability of their expression levels in the tissues and the underlying mechanism of tissue-specific expression of UGTs.

The expression profiles of UGTs in human tissues at mRNA level had been studied. However, information regarding their protein levels was limited because of the lack of isoform-specific antibodies, since UGTs share a high degree of amino acid similarities. **In chapter 2**, peptide-specific monoclonal antibodies against human UGT1A6, UGT1A8, UGT1A9, UGT1A10, UGT2B4, and UGT2B10 were prepared and were used to investigate the UGTs expression at protein levels. It was confirmed that the prepared antibodies did not cross-react with the other human UGT isoforms. Using these antibodies, it was found that UGT1A6 and UGT1A9 proteins are expressed in the kidney and the liver, but not in the small intestine, UGT2B4 and UGT2B10 are expressed only in the liver, and UGT1A10 are expressed only in the small intestine, that are consistent with previous reports of mRNA expression. In a panel of 20 individual human livers, the UGT1A6, UGT1A9, UGT2B4, and UGT2B10 protein levels exhibited 10-, 9-, 6-, and 7-fold variabilities, respectively. Their relative protein levels were not correlated with the corresponding mRNA levels, suggesting the potential importance of post-transcriptional regulation of UGT expression. An interesting finding using the prepared antibodies was that the normalized activities of recombinant UGTs were unambiguously lower than those in human tissue microsomes. Thus, differences in glucuronidation activity between recombinant UGT expression systems and human tissues

should be taken into account when predicting in vivo metabolic clearance using data from recombinant expression system. In addition, the prepared monoclonal antibodies against UGT1A6, UGT1A8, UGT1A9, UGT1A10, UGT2B4, and UGT2B10 enabled to know the distribution and relative expression levels of their proteins in human tissues.

Human UGTs show tissue-specific expression. UGT1A1 is predominantly expressed in the liver and intestine, but not in the kidney. Meanwhile UGT1A10 is exclusively expressed in the gastrointestinal tract but not in liver. **In chapters 3 and 4**, the underlying mechanism of the tissue-specific expression of UGT1A1 and UGT1A10, respectively, were investigated focusing on epigenetic mechanism. It was found that the CpG-rich region near the *UGT1A1* promoter (-85 to +40) was hypermethylated (83%) in the kidney, whereas it was hypomethylated (24%) in the hepatocytes. A chromatin immunoprecipitation assay demonstrated that histone H3 near the promoter was hypoacetylated in the kidney but was hyperacetylated in the liver; this hyperacetylation was accompanied by the recruitment of HNF1 $\alpha$  to the promoter. Thus, it was suggested that DNA hypermethylation along with histone hypoacetylation interferes with the binding of HNF1 $\alpha$ , resulting in the defective expression of UGT1A1 in the human kidney. As for UGT1A10, it was found that CpG island near the promoter (-365 to +140) was hypermethylated (89%) in the hepatocytes, whereas it was hypomethylated (6%) in the epithelium of small intestine. Reporter gene assays revealed that methylation of the *UGT1A10* promoter leads to an almost complete loss of transcriptional activity. In a UGT1A10-negative cell line, treatment with 5-Aza-dC, an inhibitor of DNA methylation, resulted in an increase of UGT1A10 mRNA expression and overexpression of HNF1 $\alpha$  and Cdx2 further increased UGT1A10 mRNA in the presence of 5-Aza-dC. A chromatin immunoprecipitation assay demonstrated that H3K27 around the promoter was trimethylated in the liver but not in the small intestine. Thus, DNA hypermethylation and H3K27 trimethylation would interfere with the binding of HNF1 $\alpha$  and Cdx2, resulting in the defective expression of UGT1A10 in the human liver. Epigenetic mechanisms are the crucial factor in the tissue-specific expression of UGTs.

In summary, this study succeeded to prepare peptide-specific monoclonal antibodies

against human UGT1A6, UGT1A8, UGT1A9, UGT1A10, UGT2B4, and UGT2B10 and could provide valuable information on the tissue distribution and interindividual variability of UGTs. In addition, it was found that the tissue-specific expression of UGTs is regulated by epigenetic mechanism including DNA methylation and histone modifications. Aging, sex, disease, and habits are known to affect epigenetic status. It would be of interest to investigate whether such factors affect drug response thorough the modulation of epigenetics of UGT.

## REFERENCES

- Aueviriyavit S, Furihata T, Morimoto K, Kobayashi K, and Chiba K (2007) Hepatocyte nuclear factor 1 alpha and 4 alpha are factors involved in interindividual variability in the expression of UGT1A6 and UGT1A9 but not UGT1A1, UGT1A3 and UGT1A4 mRNA in human livers. *Drug Metab Pharmacokinet* **22**:391-398.
- Balliet RM, Chen G, Dellinger RW, and Lazarus P (2010) UDP-glucuronosyltransferase 1A10: activity against the tobacco-specific nitrosamine, 4-(methylnitrosamino)-1-(3-pyridyl)-1-butanol, and a potential role for a novel UGT1A10 promoter deletion polymorphism in cancer susceptibility. *Drug Metab Dispos* **38**:484-490.
- Barbier O, Girard H, Inoue Y, Duez H, Villeneuve L, Kamiya A, Fruchart JC, Guillemette C, Gonzalez FJ, and Staels B (2005) Hepatic expression of the *UGT1A9* gene is governed by hepatocyte nuclear factor 4 $\alpha$ . *Mol Pharmacol* **67**:241-249.
- Basu NK, Ciotti M, Hwang MS, Kole L, Mitra PS, Cho JW, and Owens IS (2004) Differential and special properties of the major human *UGT1*-encoded gastrointestinal UDP-glucuronosyltransferases enhance potential to control chemical uptake. *J Biol Chem* **279**:1429-1441.
- Bélanger AS, Tojic J, Harvey M, and Guillemette C (2010) Regulation of *UGT1A1* and *HNF1* transcription factor gene expression by DNA methylation in colon cancer cells. *BMC Mol Biol* **11**:9.
- Bernard P, Goudonnet H, Artur Y, Desvergne B, and Wahli W (1999) Activation of the mouse TATA-less and human TATA-containing UDP-glucuronosyltransferase *1A1* promoters by hepatocyte nuclear factor 1. *Mol Pharmacol* **56**:526-536.
- Bird AP and Wolffe AP (1999) Methylation-induced repression—belts, braces, and chromatin. *Cell* **99**:451-454.
- Cameron EE, Bachman KE, Myöhänen S, Herman JG, and Baylin SB (1999) Synergy of demethylation and histone deacetylase inhibition in the re-expression of genes silenced in cancer. *Nat Genet* **21**:103-107.

- Cedar H and Bergman Y (2009) Linking DNA methylation and histone modification: patterns and paradigms. *Nat Rev Genet* **10**:295-304.
- Chou PY and Fasman GD (1974) Prediction of protein conformation. *Biochemistry* **13**:222-245.
- Court MH, Zhang X, Ding X, Yee KK, Hesse LM, and Finel M (2012) Quantitative distribution of mRNAs encoding the 19 human UDP-glucuronosyltransferase enzymes in 26 adult and 3 fetal tissues. *Xenobiotica* **42**:266-277.
- Crespi CL and Miller VP (1999) The use of heterologously expressed drug metabolizing enzymes—state of the art and prospects for the future. *Pharmacol Ther* **84**:121-131.
- Dannenberg LO and Edenberg HJ (2006) Epigenetics of gene expression in human hepatoma cells: expression profiling the response to inhibition of DNA methylation and histone deacetylation. *BMC Genomics* **7**:181.
- Emini EA, Hughes JV, Perlow DS, and Boger J (1985) Induction of hepatitis A virus-neutralizing antibody by a virus-specific synthetic peptide. *J Virol* **55**:836-839.
- Formelli F, Barua AB, and Olson JA (1996) Bioactivities of N-(4-hydroxyphenyl) retinamide and retinoyl beta-glucuronide. *FASEB J* **10**:1014-1024.
- Fujiwara R, Nakajima M, Oda S, Yamanaka H, Ikushiro S, Sakaki T, and Yokoi T (2010) Interactions between human UDP-glucuronosyltransferase (UGT) 2B7 and UGT1A enzymes. *J Pharm Sci* **99**:442-454.
- Fujiwara R, Nakajima M, Yamanaka H, Katoh M, and Yokoi T (2007a) Interactions between human UGT1A1, UGT1A4, and UGT1A6 affect their enzymatic activities. *Drug Metab Dispos* **35**:1781-1787.
- Fujiwara R, Nakajima M, Yamanaka H, Nakamura A, Katoh M, Ikushiro S, Sakaki T, and Yokoi T (2007b) Effects of coexpression of UGT1A9 on enzymatic activities of human UGT1A isoforms. *Drug Metab Dispos* **35**:747-757.
- Gaganis P, Miners JO, Brennan JS, Thomas A, and Knights KM (2007) Human renal cortical and medullary UDP-glucuronosyltransferases (UGTs): immunohistochemical localization of UGT2B7 and UGT1A enzymes and kinetic characterization of *S*-naproxen glucuronidation. *J Pharmacol Exp Ther* **323**:422-430.

- Gagnon JF, Bernard O, Villeneuve L, Têtu B, and Guillemette C (2006) Irinotecan inactivation is modulated by epigenetic silencing of *UGT1A1* in colon cancer. *Clin Cancer Res* **12**:1850-1858.
- Gardner-Stephen DA, Gregory PA, and Mackenzie PI (2005) Identification and characterization of functional hepatocyte nuclear factor 1-binding sites in UDP-glucuronosyltransferase genes. *Methods Enzymol* **400**:22-46.
- Gardner-Stephen DA and Mackenzie PI (2007) Hepatocyte nuclear factor 1 transcription factors are essential for the UDP-glucuronosyltransferase 1A9 promoter response to hepatocyte nuclear factor 4 $\alpha$ . *Pharmacogenet Genomics* **17**:25-36.
- Gardner-Stephen DA and Mackenzie PI (2008) Liver-enriched transcription factors and their role in regulating UDP glucuronosyltransferase gene expression. *Curr Drug Metab* **9**:439-452.
- Garnier J, Osguthorpe DJ, and Robson B (1978) Analysis of the accuracy and implications of simple methods for predicting the secondary structure of globular proteins. *J Mol Biol* **120**:97-120.
- Girard H, Court MH, Bernard O, Fortier LC, Villeneuve L, Hao Q, Greenblatt DJ, von Moltke LL, Perused L, and Guillemette C (2004) Identification of common polymorphisms in the promoter of the *UGT1A9* gene: evidence that *UGT1A9* protein and activity levels are strongly genetically controlled in the liver. *Pharmacogenetics* **14**:501-515.
- Girard H, Villeneuve L, Court MH, Fortier LC, Caron P, Hao Q, von Moltke LL, Greenblatt DJ, and Guillemette C (2006) The novel *UGT1A9* intronic I399 polymorphism appears as a predictor of 7-ethyl-10-hydroxycamptothecin glucuronidation levels in the liver. *Drug Metab Dispos* **34**:1220-1228.
- Gong QH, Cho JW, Huang T, Potter C, Gholami N, Basu NK, Kubota S, Carvalho S, Pennington MW, Owens IS, and Popescu NC (2001) Thirteen UDPglucuronosyltransferase genes are encoded at the human *UGT1* gene complex locus. *Pharmacogenetics* **11**:357-368.
- Gregory PA, Gardner-Stephen DA, Lewinsky RH, Duncliff KN, and Mackenzie PI (2003) Cloning and characterization of the human UDP-glucuronosyltransferase *1A8*, *1A9*, and *1A10* gene promoters: differential regulation through an interior-like region. *J Biol Chem* **278**:36107-36114.

- Gregory PA, Gardner-Stephen DA, Rogers A, Michael MZ, and Mackenzie PI (2006) The caudal-related homeodomain protein Cdx2 and hepatocyte nuclear factor 1 $\alpha$  cooperatively regulate the UDP-glucuronosyltransferase 2B7 gene promoter. *Pharmacogenet Genomics* **16**:527-536.
- Gregory PA, Lewinsky RH, Gardner-Stephen DA, and Mackenzie PI (2004a) Coordinate regulation of the human UDP-glucuronosyltransferase *1A8*, *1A9*, and *1A10* genes by hepatocyte nuclear factor 1 $\alpha$  and the caudal-related homeodomain protein 2. *Mol Pharmacol* **65**:953-963.
- Gregory PA, Lewinsky RH, Gardner-Stephen DA, and Mackenzie PI (2004b) Regulation of UDP glucuronosyltransferases in the gastrointestinal tract. *Toxicol Appl Pharmacol* **199**:354-363.
- Guillemette C (2003) Pharmacogenomics of human UDP-glucuronosyltransferase enzymes. *Pharmacogenomics J* **3**:136-158.
- Harries LW, Ellard S, Stride A, Morgan NG, and Hattersley AT (2006) Isomers of the *TCF1* gene encoding hepatocyte nuclear factor-1 alpha show differential expression in the pancreas and define the relationship between mutation position and clinical phenotype in monogenic diabetes. *Hum Mol Genet* **15**:2216-2224.
- Hawes EM (1998)  $N^+$ -glucuronidation, a common pathway in human metabolism of drugs with a tertiary amine group. *Drug Metab Dispos* **26**:830-837.
- Hopp TP and Woods KR (1981) Prediction of protein antigenic determinants from amino acid sequences. *Proc Natl Acad Sci USA* **78**:3824-3828.
- Ikushiro S, Emi Y, Kato Y, Yamada S, and Sakaki T (2006) Monospecific antipeptide antibodies against human hepatic UDP-glucuronosyltransferase 1A subfamily (UGT1A) isoforms. *Drug Metab Pharmacokinet* **21**:70-74.
- Izukawa T, Nakajima M, Fujiwara R, Yamanaka H, Fukami T, Takamiya M, Aoki Y, Ikushiro S, Sakaki T, and Yokoi T (2009) Quantitative analysis of UDP-glucuronosyltransferase (UGT) 1A and UGT2B expression levels in human livers. *Drug Metab Dispos* **37**:1759-1768.
- Jones PA and Baylin SB (2002) The fundamental role of epigenetic events in cancer. *Nat Rev Genet* **3**:415-428.

- Kato Y, Izukawa T, Oda S, Fukami T, Finel M, Yokoi T, and Nakajima M (2013) Human UGT2B10 in drug *N*-glucuronidations: substrate screening and comparison with UGT1A3 and UGT1A4. *Drug Metab Dispos* **41**:1389-1397.
- Kato Y, Nakajima M, Oda S, Fukami T, and Yokoi T (2012) Human UDP-glucuronosyltransferase isoforms involved in haloperidol glucuronidation and quantitative estimation of their contribution. *Drug Metab Dispos* **40**:240-248.
- Klose RJ and Bird AP (2006) Genomic DNA methylation: the mark and its mediators. *Trends Biochem Sci* **31**:89-97.
- Klug M and Rehli M (2006) Functional analysis of promoter CpG methylation using a CpG-free luciferase reporter vector. *Epigenetics* **1**:127-130.
- Knights KM and Miners JO (2010) Renal UDP-glucuronosyltransferases and the glucuronidation of xenobiotics and endogenous mediators. *Drug Metab Rev* **42**:63-73.
- Krishnaswamy S, Duan SX, Von Moltke LL, Greenblatt DJ, and Court MH (2003) Validation of serotonin (5-hydroxytryptamine) as an in vitro substrate probe for human UDP-glucuronosyltransferase (UGT) 1A6. *Drug Metab Dispos* **31**:133-139.
- Krishnaswamy S, Hao Q, Al-Rohaimi A, Hesse LM, von Moltke LL, Greenblatt DJ, and Court MH (2005) UDP glucuronosyltransferase (UGT) 1A6 pharmacogenetics: II. Functional impact of the three most common nonsynonymous UGT1A6 polymorphisms (S7A, T181A, and R184S). *J Pharmacol Exp Ther* **313**:1340-1346.
- Kubicek S, O'Sullivan RJ, August EM, Hickey ER, Zhang Q, Teodoro ML, Rea S, Mechtler K, Kowalski JA, Homon CA, Kelly TA, and Jenuwein T (2007) Reversal of H3K9me2 by a small-molecule inhibitor for the G9a histone methyltransferase. *Mol Cell* **25**:473-481.
- Kumaki Y, Oda M, and Okano M (2008) QUMA: quantification tool for methylation analysis. *Nucleic Acids Res* **36**:W170-175.
- Mackenzie PI, Bock KW, Burchell B, Guillemette C, Ikushiro S, Iyanagi T, Miners JO, Owens IS, and Nebert DW (2005) Nomenclature update for the mammalian UDP glycosyltransferase (UGT) gene superfamily. *Pharmacogenet Genomics* **15**:677-685.

- Mackenzie PI, Gregory PA, Gardner-Stephen DA, Lewinsky RH, Jorgensen BR, Nishiyama T, Xie W, and Radominska-Pandya A (2003) Regulation of UDP glucuronosyltransferase genes. *Curr Drug Metab* **4**:249-257.
- Mackenzie PI, Hu DG, and Gardner-Stephen DA (2010) The regulation of UDP-glucuronosyltransferase genes by tissue-specific and ligand-activated transcription factors. *Drug Metab Rev* **42**:99-109.
- Miners JO, Knights KM, Houston JB, and Mackenzie PI (2006) In vitro-in vivo correlation for drugs and other compounds eliminated by glucuronidation in humans: pitfalls and promises. *Biochem Pharmacol* **71**:1531-1539.
- Mizuma T (2009) Intestinal glucuronidation metabolism may have a greater impact on oral bioavailability than hepatic glucuronidation metabolism in humans: a study with raloxifene, substrate for UGT1A1, 1A8, 1A9, and 1A10. *Int J Pharm* **378**:140-141.
- Nakajima M, Koga T, Sakai H, Yamanaka H, Fujiwara R, and Yokoi T (2010) N-Glycosylation plays a role in protein folding of human UGT1A9. *Biochem Pharmacol* **79**:1165-1172.
- Nakajima M, Tanaka E, Kwon JT, and Yokoi T (2002) Characterization of nicotine and cotinine N-glucuronidations in human liver microsomes. *Drug Metab Dispos* **30**:1484-1490.
- Nakajima M and Yokoi T (2011) MicroRNAs from biology to future pharmacotherapy: regulation of cytochrome P450s and nuclear receptors. *Pharmacol Ther* **131**:330-337.
- Nakamura A, Nakajima M, Yamanaka H, Fujiwara R, and Yokoi T (2008) Expression of UGT1A and UGT2B mRNA in human normal tissues and various cell lines. *Drug Metab Dispos* **36**:1461-1464.
- Oda S, Fukami T, Yokoi T, and Nakajima M. Epigenetic regulation is a crucial factor in the repression of UGT1A1 expression in the human kidney. *Drug Metab Dispos*, in press.
- Ohgane J, Yagi S, and Shiota K (2008) Epigenetics: the DNA methylation profile of tissue-dependent and differentially methylated regions in cells. *Placenta* **29 Suppl A**:S29-35.
- Ohno S and Nakajin S (2009) Determination of mRNA expression of human UDP-glucuronosyltransferases and application for localization in various human tissues by real-time reverse transcriptase-polymerase chain reaction. *Drug Metab Dispos* **37**:32-40.

- Ohtsuki S, Schaefer O, Kawakami H, Inoue T, Liehner S, Saito A, Ishiguro N, Kishimoto W, Ludwig-Schwellinger E, Ebner T, and Terasaki T (2012) Simultaneous absolute protein quantification of transporters, cytochromes P450, and UDP-glucuronosyltransferases as a novel approach for the characterization of individual human liver: comparison with mRNA levels and activities. *Drug Metab Dispos* **40**:83-92.
- Parker JM, Guo D, and Hodges RS (1986) New hydrophilicity scale derived from high-performance liquid chromatography peptide retention data: correlation of predicted surface residues with antigenicity and X-ray-derived accessible sites. *Biochemistry* **25**:5425-5432.
- Pillot T, Ouzzine M, Fournel-Gigleux S, Lafaurie C, Radomska A, Burchell B, Siest G, and Magdalou J (1993) Glucuronidation of hyodeoxycholic acid in human liver. Evidence for a selective role of UDP-glucuronosyltransferase 2B4. *J Biol Chem* **268**:25636-25642.
- Portela A and Esteller M (2010) Epigenetic modifications and human disease. *Nat Biotechnol* **28**:1057-1068.
- Ramírez J, Mirkov S, Zhang W, Chen P, Das S, Liu W, Ratain MJ, and Innocenti F (2008) Hepatocyte nuclear factor-1 alpha is associated with *UGT1A1*, *UGT1A9* and *UGT2B7* mRNA expression in human liver. *Pharmacogenomics J* **8**:152-161.
- Reddington JP, Pennings S, and Meehan RR (2013) Non-canonical functions of the DNA methylome in gene regulation. *Biochem J* **451**:13-23.
- Rey-Campos J, Chouard T, Yaniv M, and Cereghini S (1991) vHNF1 is a homeoprotein that activates transcription and forms heterodimers with HNF1. *EMBO J* **10**:1445-1457.
- Ritter JK (2000) Roles of glucuronidation and UDP-glucuronosyltransferases in xenobiotic bioactivation reactions. *Chem Biol Interact* **129**:171-193.
- Ritter JK (2007) Intestinal UGTs as potential modifiers of pharmacokinetics and biological responses to drugs and xenobiotics. *Expert Opin Drug Metab Toxicol* **3**:93-107.
- Ritter JK, Yeatman MT, Ferreira P, and Owens IS (1992) Identification of a genetic alteration in the code for bilirubin UDP-glucuronosyltransferase in the *UGT1* gene complex of a Crigler-Najjar type I patient. *J Clin Invest* **90**:150-155.

- Senekeo-Effenberger K, Chen S, Brace-Sinnokrak E, Bonzo JA, Yueh MF, Argikar U, Kaeding J, Trottier J, Rimmel RP, Ritter JK, Barbier O, and Tukey RH (2007) Expression of the human UGT1 locus in transgenic mice by 4-chloro-6-(2,3-xylydino)-2-pyrimidinylthioacetic acid (WY-14643) and implications on drug metabolism through peroxisome proliferator-activated receptor  $\alpha$  activation. *Drug Metab Dispos* **35**:419-427.
- Sharma S, Kelly TK, and Jones PA (2010) Epigenetics in cancer. *Carcinogenesis* **31**:27-36.
- Shimomura K, Kamata O, Ueki S, Ida S, and Oguri K (1971) Analgesic effect of morphine glucuronides. *Tohoku J Exp Med* **105**:45-52.
- Shiota K (2004) DNA methylation profiles of CpG islands for cellular differentiation and development in mammals. *Cytogenet Genome Res* **105**:325-334.
- Simon JA and Kingston RE (2009) Mechanisms of polycomb gene silencing: knowns and unknowns. *Nat Rev Mol Cell Biol* **10**:697-708.
- Starlard-Davenport A, Lyn-Cook B, and Radomska-Pandya A (2008) Identification of UDP-glucuronosyltransferase 1A10 in non-malignant and malignant human breast tissues. *Steroids* **73**:611-620.
- Strassburg CP, Kneip S, Topp J, Obermayer-Straub P, Barut A, Tukey RH, and Manns MP (2000) Polymorphic gene regulation and interindividual variation of UDP-glucuronosyltransferase activity in human small intestine. *J Biol Chem* **275**:36164-36171.
- Strassburg CP, Manns MP, and Tukey RH (1998a) Expression of the UDP-glucuronosyltransferase 1A locus in human colon. Identification and characterization of the novel extrahepatic UGT1A8. *J Biol Chem* **273**:8719-8726.
- Strassburg CP, Nguyen N, Manns MP, and Tukey RH (1998b) Polymorphic expression of the UDP-glucuronosyltransferase *UGT1A* gene locus in human gastric epithelium. *Mol Pharmacol* **54**:647-654.
- Strassburg CP, Oldhafer K, Manns MP, and Tukey RH (1997) Differential expression of the *UGT1A* locus in human liver, biliary, and gastric tissue: identification of *UGT1A7* and *UGT1A10* transcripts in extrahepatic tissue. *Mol Pharmacol* **52**:212-220.

- Sugatani J, Mizushima K, Osabe M, Yamakawa K, Kakizaki S, Takagi H, Mori M, Ikari A, and Miwa M (2008) Transcriptional regulation of human *UGT1A1* gene expression through distal and proximal promoter motifs: implication of defects in the *UGT1A1* gene promoter. *Naunyn Schmiedebergs Arch Pharmacol* **377**:597-605.
- Sutherland L, Ebner T, and Burchell B (1993) The expression of UDP-glucuronosyltransferases of the UGT1 family in human liver and kidney and in response to drugs. *Biochem Pharmacol* **45**:295-301.
- Tabata T, Katoh M, Tokudome S, Hosakawa M, Chiba K, Nakajima M, and Yokoi T (2004) Bioactivation of capecitabine in human liver: involvement of the cytosolic enzyme on 5'-deoxy-5-fluorocytidine formation. *Drug Metab Dispos* **32**:762-767.
- Takagi S, Nakajima M, Kida K, Yamaura Y, Fukami T, and Yokoi T (2010) MicroRNAs regulate human hepatocyte nuclear factor 4 $\alpha$ , modulating the expression of metabolic enzymes and cell cycle. *J Biol Chem* **285**:4415-4422.
- Tan J, Yang X, Zhuang L, Jiang X, Chen W, Lee PL, Karuturi RK, Tan PB, Liu ET, and Yu Q (2007) Pharmacologic disruption of Polycomb-repressive complex 2-mediated gene repression selectively induces apoptosis in cancer cells. *Genes Dev* **21**:1050-1063.
- Usui T, Kuno T, Ueyama H, Ohkubo I, and Mizutani T (2006) Proximal HNF1 element is essential for the induction of human UDP-glucuronosyltransferase 1A1 by glucocorticoid receptor. *Biochem Pharmacol* **71**:693-701.
- Valentini A, Biancolella M, Amati F, Gravina P, Miano R, Chillemi G, Farcomeni A, Bueno S, Vespasiani G, Desideri A, Federici G, Novelli G, and Bernardini S (2007) Valproic acid induces neuroendocrine differentiation and UGT2B7 up-regulation in human prostate carcinoma cell line. *Drug Metab Dispos* **35**:968-972.
- Viré E, Brenner C, Deplus R, Blanchon L, Fraga M, Didelot C, Morey L, Van Eynde A, Bernard D, Vanderwinden JM, Bollen M, Esteller M, Di Croce L, de Launoit Y, and Fuks F (2006) The Polycomb group protein EZH2 directly controls DNA methylation. *Nature* **439**:871-874.
- Welling GW, Weijer WJ, van der Zee R, and Welling-Wester S (1985) Prediction of sequential antigenic regions in proteins. *FEBS Lett* **188**:215-218.

- Yueh MF, Huang YH, Hiller A, Chen S, Nguyen N, and Tukey RH (2003) Involvement of the xenobiotic response element (XRE) in Ah receptor-mediated induction of human UDP-glucuronosyltransferase *1A1*. *J Biol Chem* **278**:15001-15006.
- Yueh MF and Tukey RH (2007) Nrf2-Keap1 signaling pathway regulates human UGT1A1 expression *in vitro* and in transgenic *UGT1* mice. *J Biol Chem* **282**:8749-8758.
- Zhu L, Ge G, Zhang H, Liu H, He G, Liang S, Zhang Y, Fang Z, Dong P, Finel M, and Yang L (2012) Characterization of hepatic and intestinal glucuronidation of magnolol: application of the relative activity factor approach to decipher the contributions of multiple UDP-glucuronosyltransferase isoforms. *Drug Metab Dispos* **40**:529-538.

## LIST OF PUBLICATIONS

### Main publications

1. **Oda S**, Nakajima M, Hatakeyama M, Fukami T, and Yokoi T (2012) Preparation of a specific monoclonal antibody against human UGT1A9 and evaluation of UGT1A9 protein levels in human tissues. *Drug Metab Dispos* **40**:1620-1627.
2. **Oda S**, Fukami T, Yokoi T, and Nakajima M. Epigenetic regulation is a crucial factor in the repression of UGT1A1 expression in the human kidney. *Drug Metab Dispos*, in press.

### Supplemental publications

1. Fujiwara R, Nakajima M, **Oda S**, Yamanaka H, Ikushiro S, Sakaki T, and Yokoi T (2010) Interactions between human UDP-glucuronosyltransferase (UGT) 2B7 and UGT1A enzymes. *J Pharm Sci* **99**:442-454.
2. Abe Y, Fujiwara R, **Oda S**, Yokoi T, and Nakajima M (2011) Interpretation of the effects of protein kinase C inhibitors on human UDP-glucuronosyltransferase 1A (UGT1A) proteins *in cellulo*. *Drug Metab Pharmacokinet* **26**:256-265.
3. **Oda S**, Nakajima M, Toyoda Y, Fukami T, and Yokoi T (2011) Progesterone receptor membrane component 1 modulates human cytochrome P450 activities in an isoform-dependent manner. *Drug Metab Dispos* **39**:2057-2065.
4. Kato Y, Nakajima M, **Oda S**, Fukami T, and Yokoi T (2012) Human UDP-glucuronosyltransferase isoforms involved in haloperidol glucuronidation and quantitative estimation of their contribution. *Drug Metab Dispos* **40**:240-248.
5. Kato Y, Izukawa T, **Oda S**, Fukami T, Finel M, Yokoi T, and Nakajima M (2013) Human UGT2B10 in drug *N*-glucuronidations: substrate screening and comparison with UGT1A3 and UGT1A4. *Drug Metab Dispos* **41**:1389-1397.

## ACKNOWLEDGEMENTS

I would like to express my deepest appreciation and sincere gratitude to Associate Professor Dr. Miki Nakajima and Professor Dr. Tsuyoshi Yokoi for their excellent supervision guidance and constructive criticism throughout my research until the accomplishment of this Ph.D. thesis. I greatly appreciate Professor Dr. Yukio Kato, Associate Professors Dr. Takeo Nakanishi, and Dr. Yoshimichi Sai for valuable comments and suggestions as reviewers.

I am grateful to Drs. Yasuhiro Aoki (Iwate Medical University, Japan) and Michael Rehli (University Hospital Regensburg, Germany) for providing human tissue samples and the pCpGL-basic plasmid, respectively. I am also grateful to Mr. Masahiko Hatakeyama (CLEA Japan, Inc., Japan) for the help to prepare monoclonal antibodies and giving valuable advice.

Finally, I wish to express thanks to Ms. Yukiko Kato for kind advices during this study. I wish to extend my thanks to all members of Division of Drug Metabolism and Toxicology, Kanazawa University, my family, and friends for helping out and being supportive throughout my studies at Kanazawa University.